Lithos 262 (2016) 398–427

Contents lists available at ScienceDirect

Lithos

journal homepage: www.elsevier.com/locate/lithos

Invited review article

Radiogenic heat production in the continental crust

Claude Jaupart [a], Jean-Claude Mareschal [b,*], Lidia Iarotsky [b]

[a] Institut de Physique du Globe de Paris, Sorbonne Paris Cité, Université Paris Diderot, CNRS (UMR 7154), France
[b] GEOTOP, University of Quebec, Montreal, Canada

ARTICLE INFO

Article history:
Received 29 April 2016
Accepted 12 July 2016
Available online 25 July 2016

Keywords:
Cratons
Heat flow
Crustal heat production
Crustal evolution
High temperature metamorphism
Post-orogenic metamorphism

ABSTRACT

The thermal structure and evolution of continents depend strongly on the amount and distribution of radioactive heat sources in the crust. Determining the contribution of crustal rocks beneath a superficial layer is a major challenge because heat production depends weakly on major element composition and physical properties such as seismic wavespeed and density. Enriched granitic intrusives that lie at the current erosion level have a large impact on the surface heat flux but little influence on temperatures in the deep crust. Many lower crustal rocks that are poor in heat producing elements are restites from ancient orogenic events, implying that enrichment of the upper crust was achieved at the expense of deeper crustal levels. For the same total heat production, concentrating heat sources in an upper layer acts to reduce temperatures in the lower crust, thereby allowing stabilization of the crust. The present-day structure of the crust is a consequence of orogeny and should not be adopted for thermal models of the orogenic event itself.

This review summarizes information extracted from large data sets on heat flow and heat production and provides estimates of crustal stratification and heat production in several geological provinces. Analysis of global and regional data sets reveals the absence of a positive correlation between surface heat flow and crustal thickness, showing that the average crustal heat production is not constant. Differences of heat flow between geological provinces are due in large part to changes of crustal structure and bulk composition. Collating values of the bulk crustal heat production in a few age intervals reveals a clear trend of decrease with increasing age. This trend can be accounted for by radioactive decay, indicating that thermal conditions at the time of crustal stabilization have not changed significantly. For the average crustal thickness of 40 km, Moho temperatures are near solidus values at the time of stabilization, suggesting an intrinsic thermal control on crustal thickness and heat production distribution. Crustal thickening by more than about 10 km above this mean value induces changes of gravitational potential energy that exceed the strength of the lithosphere.

For several provinces where strong constraints on heat production are available, it is shown that, prior to intracrustal fractionation, only modest amounts of thickening were needed to generate the conditions of ultrahigh temperature metamorphism. The tell-tale signature of crustal heat production is anatectic and metamorphic events that lag the cessation of orogenic activity by several tens of million years.

Crustal heat production is decreasing with time because it is due to the radioactive decay of Uranium Thorium and Potassium. Its rundown is responsible for the secular cooling of lithospheric roots at a typical rate of about 100 K Gy $^{-1}$, implying complex thermal interactions with a convecting mantle that is not cooling at the same rate.

Contents

* Corresponding author at: GEOTOP, University of Quebec, Montreal, POB 8888, sta. "downtown", Montreal, QC, H3C3P8, Canada.
E-mail addresses: mareschal.jean-claude@uqam.ca, jeanclaude.mareschal@gmail.com (J.-C. Mareschal).

http://dx.doi.org/10.1016/j.lithos.2016.07.017
0024-4937/

1. Introduction

The formation and stabilization of continental crust are key features of the Earth's geodynamic cycle. Conventionally, this is described as a one-way process, such that continental material is extracted from the mantle and stored at the top of rigid lithosphere. It is now clear, however, that crustal processes may also affect the Earth's mantle. The bulk composition of continental crust is close to that of an andesite and yet its parent melts are basaltic, which indicates that crustal fractionation processes involve the separation of a felsic fraction from mafic residues that are returned to the mantle (Arndt and Goldstein, 1989; Kelemen et al., 2014; Rudnick and Gao, 2014). Thus, the composition of continental crust provides information not only on the origin and evolution of continents but also on planetary-scale processes. This is especially true for the concentrations of the main heat producing elements, Uranium and Thorium. Because they are strongly incompatible, these elements get concentrated in continental crust with two types of consequences. On a global scale, this depletes the convecting mantle of its heat sources with implications for the Earth's thermal evolution and secular cooling (Jaupart and Mareschal, 2011). On a local scale, this is responsible for thermal regimes that are intrinsic to continents with external processes that may play only a relatively minor role. Amongst the many characteristics that make continental crust distinctive and different from the Earth's mantle, radiogenic heat production may be the most multifaceted because it is at the same time a tracer of petrological/tectonic processes and a key geophysical variable. In spite of its importance, its total amount in continents remains poorly constrained, with large uncertainties on the contribution of deep crustal levels. It has been argued recently, for example, that the lower crust is less depleted than previously thought due to the relamination of felsic gneisses in subduction zones (Hacker et al., 2011).

The fundamental uncertainty on the amount and vertical distribution of heat production weighs on the validity of physical models of geological phenomena. These models have become increasingly detailed in the last few decades and have been used to account for the timing and characteristics of thermal events as well as for the rates of tectonic deformation. Their outputs critically depend on thermal structure and evolution. Our purpose is not to provide a comprehensive overview of such models past and present but to point out that thermal properties and variables have received much less attention than geodynamic processes such as mantle plumes and lithospheric instabilities for example. Thus, there has been a tendency to attribute the failure of a model to an erroneous geodynamic setting rather than to incorrect choices of physical parameters. In this context, it is worth emphasizing the fundamental difference between properties such as thermal conductivity and heat capacity on the one hand and radiogenic heat production on the other hand. The former are intrinsic mineral properties that are independent of the geological setting. They vary within restricted ranges and can be specified with little error without detailed knowledge of local conditions. The latter, in contrast, depends weakly on rock type and major element composition and must be determined on a case by case basis (Fountain, 1986; Kukkonen and Peltoniemi, 1998; Slagstad, 2008).

There can be no doubt that heat released by radioactive decay in crustal rocks accounts for a large fraction of the surface heat flux and strongly affects the thermal regimes of both crust and lithosphere (England and Thompson, 1984; Jaupart et al., 1998; Mareschal and Jaupart, 2013; Sandiford et al., 2002). In spite of this, heat production data are rarely considered as an important part of geophysical studies and are not systematically collected with heat flow measurements. For example, a global compilation of heat flow data contains more than 17,000 conventional heat flow measurements on land but only 1785 of these are associated with heat production values. Such a dearth of

heat production measurements has been circumvented in different ways, as will be shown in this paper, but this has prevented robust conclusions on the thermal conditions of many geological events. For example, there is still no consensus on what causes the ultrahigh temperature metamorphism (900–1000 °C) that has affected many geological provinces (Heaman et al., 2011). A dominant role for crustal heat sources has been advocated in a few cases (Chamberlain and Sonder, 1990; Jaupart and Mareschal, 2015b; Kramers et al., 2001; McLaren et al., 2006), but this idea has not enjoyed wide acceptance. Another example is the focusing of intracratonic deformation caused by far field stresses or lithospheric mantle instabilities, which has been attributed to two effects. One is a tectonic fabric inherited from older rifting events which manifests itself as lattice preferred orientation of mantle olivine crystals (Tommasi and Vauchez, 2001; Vauchez et al., 1998). An alternative effect is a local reduction in lithospheric strength caused by high crustal heat production (Burov et al., 1998; Pysklywec and Beaumont, 2004; Sandiford and Hand, 1998).

Determining the rate of crustal heat production in a geological province has proven to be a major scientific challenge because continental crust is the end result of a complex sequence of processes. Crustal material is extracted from the mantle through melting in a variety of settings and gets accreted to the margins of older nuclei in piecemeal fashion. Once it has been incorporated in a continent, a juvenile terrane may be subjected to later magmatic, metamorphic and tectonic events that modify it comprehensively. In addition, parts of it get redistributed by erosion and sediment deposition. Concentrations in heat producing elements are also affected by alteration processes. As a consequence, the composition and vertical structure of continental crust do not conform to a single universal model and exhibit considerable variety amongst geological provinces.

In this paper, we gather a large amount of data from representative geological provinces throughout the world and provide a review of crustal heat production and its impact on the thermal structure and evolution of continental crust. We limit ourselves to a few issues. Can crustal heat production account for some of the thermal events that affect continental crust, such as high-T metamorphism for example? What information is required for a reliable thermal model and what can be done if this information is not directly available? What are the scales and magnitudes of lateral variations of heat production in a geological province? For reference, we begin by reviewing geochemical models focussing on the vertical stratification of the crust and heat production in the lower crust. We then discuss the required inputs for thermal models of the crust and lithosphere, focussing on how they can be retrieved from an analysis of heat flow data. We show that, with adequate heat flux and heat production data coverage, it may be possible to identify different types of crust and evaluate their stratification degrees. This allows calculations of thermal structure and evolution that are reliable enough for most practical purposes. The data emphasize that heat flow and crustal heat production both vary laterally by large amounts, even within a single geological province. These variations may occur on a large scale, with enriched belts at the boundaries of older continental blocks, with important implications for the mechanical behaviour of continents. In a last section, we summarize a few important facts about the transient thermal evolution of continents and describe a few telltale effects of crustal heat production.

2. Geochemical models of the continental crust

Continental crustal material is extracted from the mantle in subduction zones and hot spot environments. Extraction is followed by a magmatic phase which includes fractional crystallization and the separation of felsic melts from mafic residues. It has long been recognized that the bulk continental crust differs significantly from its parent melts. Almost all mantle-derived magmas are basaltic, whereas the average continental crust is closer to an andesite (Kelemen et al., 2014; Rudnick and Gao, 2014; Taylor, 1977; Taylor and McLennan, 1995). Several mechanisms

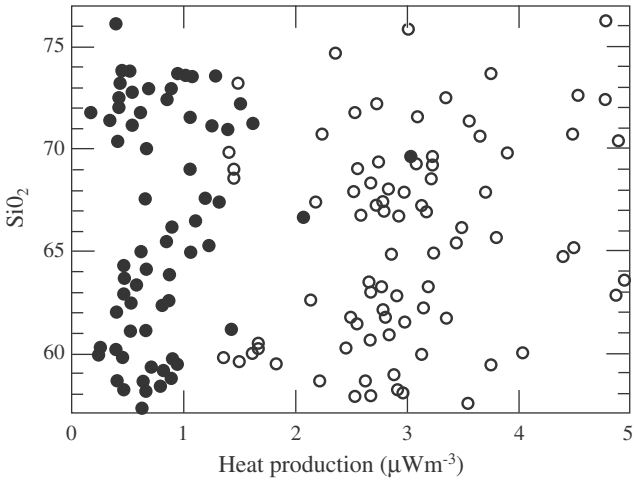

Fig. 1. Radiogenic heat production rate as a function of SiO_2 content in % in the Sierra Nevada batholith, from data in Sawka and Chappell (1988). Filled circles: western foothills tonalites–trondhjemites. Open circles: granitoids from the central and eastern parts of the batholith.

have been invoked, including delamination of dense mafic cumulates and relamination of felsic gneisses to the base of the crust (Hacker et al., 2015). Which mechanism dominates has major consequences that go far beyond petrological and geochemical interests. Should the relamination model be valid, a significant fraction of the lower crust would be made of felsic rocks with higher heat production than mafic ones.

A big stumbling block is that radiogenic heat production cannot be related in any meaningful way to major element composition on the one hand and bulk physical properties such as density and seismic velocities on the other hand (Figs. 1–2). Thus, one cannot readily convert geophysical or petrological information into constraints on crustal heat sources. This is of particular concern for the lower crust because, as we shall see, it has a major impact on the thermal structure of continents.

One could hope to determine the crustal structure directly by studying exposed vertical cross-sections, but they are rare and seldom complete. Outcrops of rocks that have equilibrated over the whole range of crustal pressures and that reach into mantle peridotites have been

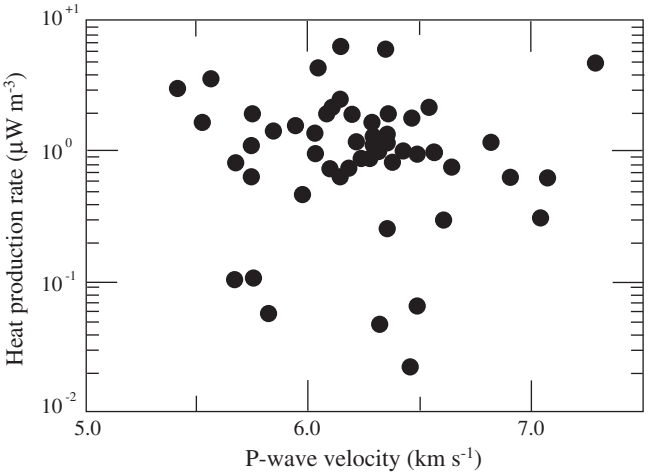

Fig. 2. Radiogenic heat production rate as a function of P-wave velocity in Precambrian granulite-facies rocks from Finland and Estonia, from data in Joeleht and Kukkonen (1998).

studied in two areas, Talkeetna, Alaska, and Kohistan, Pakistan (Hacker et al., 2008; Jagoutz, 2010; Jagoutz and Schmidt, 2012). Both were oceanic volcanic arcs but have bulk major element contents that are close to those of the continental crust. Unfortunately, the Talkeetna lack substantial outcrops of mid-crustal plutonic rocks. One other crustal cross-section was reconstructed in the North American Cordillera using thick batholithic sequences that span upper and middle crustal pressure ranges and xenoliths from the lower crust (Lee et al., 2007). Xenolith populations, however, may not be fully representative of average continental crust because their carrier basaltic magmas cannot go through thick felsic environments that are less dense than them. There may thus be a sampling bias in favour of mafic rocks. With due caution for this, the North American Cordillera provides us with a section through a continental volcanic arc, which complements the oceanic ones from Alaska and Pakistan.

Table 1 lists recent models for the continental crust, including global ones based on large geochemical data sets and the two complete vertical cross-sections that have been described above. In order to derive a crustal model from geochemical data, one must separate the crust into components (layers in practice) with distinctive physical properties and chemical compositions. Following global seismic syntheses, the crystalline part of the crust is split into three layers (Bassin et al., 2000; Mooney et al., 1998). Huang et al. (2013) included continental shelves and rifts to define a global average crust with 34 km thickness. Rudnick and Gao (2014) and Hacker et al. (2015) took shields and platforms only, with total crustal thicknesses of 40 and 39 km, respectively. The composition of the upper layer was derived from surface sample compilations and is nearly the same in the three global models (Table 1). The other two layers were assigned compositions on the basis of their densities and seismic wavespeeds. Hacker et al. (2015) allowed for different end-members, leading to four alternative models (Table 1). For the crustal cross-sections, layer thicknesses were derived from metamorphic barometric data and field measurements. The latter may not be fully representative due to syn-emplacement deformation and thrusting, which led Jagoutz and Schmidt (2012) to propose three different alternatives.

Table 1
Different estimates of heat production in the continental crust (in μW m^{-3}). For each crustal model with the exception of the North American cordillera, the first line lists the thicknesses of the crustal layers and the total crust thickness.

Model	Upper crust	Middle crust	Lower crust	Bulk
Global geochemical models				
Rudnick and Gao (2014)	12 km	11 km	17 km	40 km
	1.6	0.96	0.18	0.89
Huang et al. (2013)	13 km	11 km	10 km	34 km
	1.6	0.73	0.17	0.94
Hacker et al. (2015)[a]	13.7 km	13 km	12.1 km	38.8 km
Model A	1.58	0.35	0.21	0.74
Model B	1.58	0.34	0.17	0.72
Model C	1.58	0.46	0.26	0.80
Model D	1.58	0.72	0.33	0.90
Exposed cross-sections				
North American Cordillera				
Lee et al. (2007)[b]	1.67	0.99	0.2	0.88
Kohistan, Pakistan				
Jagoutz and Schmidt (2012)[c]	/	/	≈25 km	≈55 km
Model 1	/	/	0.18	0.69
Model 2	/	/	0.11	0.50
Model 3	/	/	0.06	0.58
Heat flow data				
Jaupart and Mareschal (2014)				0.79–0.95

[a] Models A–D correspond to different end-member compositions that are compatible with geophysical characteristics.
[b] No thicknesses for the three crustal layers are reported.
[c] Models 1–3 correspond to slightly different thicknesses and the inclusion or exclusion of the Chilas ultramafic–mafic complex.

There is little disagreement between the crustal models of Table 1. Heat production values for the Kohistan oceanic volcanic arc are significantly smaller than those of all the other entries. The bulk heat production of the American Cordillera continental arc falls within the range of the "global" geochemical models. For our present purposes, it is significant that these models are consistent with heat flow data constraints (Table 1).

The global crustal models rely on both geochemical and geophysical data. For expediency reasons, geophysical constraints have been collapsed into a few type-structures involving a small number of crustal layers (Bassin et al., 2000; Mooney et al., 1998), which gloss over the complex architecture of continents. For example, it is not clear how one can go from the detailed seismic models of the Western Superior Province (Musacchio et al., 2004), which emphasize crustal-scale low-angle thrusts and across-strike fabric variations, to a single layered structure. Some "averaging" process has been applied to the data at a scale which is not well-defined and which may not be consistent with the requirements of thermal models. The issue of the proper scale forms one of the major themes of this paper.

The crustal models of Table 1 were designed to address geochemical and petrological problems and provide indispensable references. For heat flow studies, however, they suffer from several important shortcomings. The most critical one is certainly that they are generic models that cannot be applied to any particular province. They do not inform about the large horizontal variations of crustal structure and composition that exist within a province. They correspond to a worldwide average crustal thickness and it is not clear how they can be extended to crusts that are thicker or thinner than average. In the Archean Superior Province, for example, crustal thickness varies between 35 and 55 km (Perry et al., 2002). Yet another shortcoming is that the spread of heat production values that is allowed is too large for comfort. Estimates of the bulk crustal heat production vary within a 0.75–0.93 μW m^{-3} range and get amplified when they are extrapolated back in time. In studies of the Archean, for example, one must correct for radioactive decay over more than 2.5 Gy, which increases heat production values by a factor of at least two. The wider spread of heat production values that is induced allows for a large temperature range of about 200 °C in the deep crust in Archean time.

3. Thermal models of the continental crust: inputs and uncertainties

In this section, we illustrate the importance of crustal heat production for thermal models of continents and discuss the consequences of lateral and vertical variations of heat production. For this purpose, we use steady-state models because transient phenomena cannot be studied in a generic manner and must be evaluated on a case-by-case basis. Further, we take thermal conductivity to be constant. As shown in Appendix A, using an average value of thermal conductivity (≈2.1 W m^{-1} K^{-1}), provided that it is chosen properly, results in negligible errors on Moho temperature. These two assumptions, which will be relaxed in other sections, allow a clear separation of the various effects that come into play.

Temperatures in the crust are solutions of the heat equation:

$$\lambda \nabla^2 T + A = 0 \quad (1)$$

where λ is the thermal conductivity and A is the heat production rate. Two boundary conditions are needed. One states that the surface temperature T_0 is constant (= 0) and the other one deals with the heat flux at the surface, q_0, or at the Moho, q_m. The former is taken from field measurements and the latter may be inferred from the systematics of heat flow and heat production data as well as from several independent constraints, as discussed in Appendix B. One must also specify the vertical distribution of heat production in the crust.

It is useful to decompose the temperature field into a horizontal average and a fluctuation, such that $T = \overline{T} + \delta T$. The heat equation may then be split into two equations, one for each component:

$$\begin{aligned} \lambda \frac{d^2\overline{T}}{dz^2} + \overline{A}(z) &= 0 \\ \lambda \nabla^2 \delta T + \delta A(x,y,z) &= 0 \end{aligned} \tag{2}$$

where $\overline{A}$ is the horizontally-averaged heat production, which may vary only as a function of depth z, and δA describes the horizontal variations of heat production around the mean.

3.1. The total amount of heat produced in the crust

Here, we deal with average values in a province, such that the horizontally-averaged heat flux is:

$$\overline{q_0} = q_m + \int_0^{h_m} \overline{A} dz = q_m + q_c \tag{3}$$

where q_m is the Moho heat flux, h_m is the Moho depth, and q_c is the contribution of crustal sources to the heat flux, which shall be called the crustal heat flow component.

One should note that, in the above equation, the Moho heat flux has not been written as a horizontal average. Ignoring radioactive sources within the lithospheric mantle, whose contributions can only be small (Jaupart and Mareschal, 1999; Michaut et al., 2007), the Moho heat flux is equal to the rate of heat supply from the asthenosphere, which will be called the mantle heat flux. The base of the lithosphere lies at depths of 150 km or more beneath stable geological provinces, implying that lateral variations of the mantle heat flux at scales of 500 km or less are effectively smoothed out by horizontal heat transport (Mareschal and Jaupart, 2004). This cut-off scale can be as large as 800 km for the Archean lithosphere that is 250 km-thick. Thus, in a geological province, the Moho heat flux can be taken as uniform for all practical purposes, implying that lateral variations of the surface heat flux can only be due to crustal heat sources. This separation of scales can be turned to one's advantage when one is interpreting heat flow data. We review in Appendix B various methods that have been used to calculate the Moho heat flux. They all converge to a narrow range of 12–18 mW m^{-2}, which will be used throughout the following. This is less than estimates that have been used in many past studies, with important implications for the thermal regime of the crust.

For homogeneous crust, $q_c = A_c h_m$ and the temperature at Moho T_m is:

$$T_m = T_0 + \frac{q_c}{2\lambda} h_m + \frac{q_m}{\lambda} h_m \tag{4}$$

where the first term represents the contribution of crustal heat production to Moho temperature and the second is the contribution of the mantle heat flux. For Archean cratons today, $q_0 = 42$ mW m^{-2} and $q_m = 15$ mW m^{-2} (Jaupart and Mareschal, 1999), so that $q_c = 27$ mW m^{-2}. Thus, the crustal and mantle contributions to the Moho temperature are about equal today. In Archean times, accounting for radioactive decay, q_c had to be at least twice as large as present (>54 mW m^{-2}), implying that the Moho temperature was higher unless the mantle heat flux was negative. We discuss below how to obtain estimates of the paleo mantle heat flux and how they can be related to the lithosphere thickness. Regardless of the uncertainties involved, a negative mantle heat flux is highly unlikely and we conclude that crustal temperatures were higher in Archean cratons when they stabilized. We shall see that the Archean continental thermal regime was in fact not very different from today.

The assumption of a homogeneous crust is not tenable in many provinces because the surface heat production is much larger than the crustal average. This is usually associated with the presence of evolved granitic rocks with high concentrations of uranium and thorium. For the same total heat production, a crust that is stratified vertically in this manner has much lower temperatures than a homogeneous one. Information on the vertical distribution of heat production is therefore required for a reliable thermal model. One should be aware, however, that this vertical distribution was established at some time in the past and is not appropriate for earlier events. In many provinces, for example, enriched granitic plutons that now lie in the upper crust were intruded in the midst or after the end of orogenic activity, implying that the present-day distribution of heat production is not relevant to the orogenic event itself.

3.2. Sensitivity of the Moho temperature to the depth of heat sources

Here, we show that an enriched upper crust has little impact on temperatures in the lower crust. We consider a crust made up of three layers such as shown in Table 1. The lowermost crust has heat production A_0, the enriched upper crust has heat production $A_1 = A_0 + \Delta A$. For our present purpose we need only to calculate the contribution of the background crustal heat production A_0 over the entire crustal thickness h_m, and the effect of the enrichment of the upper crustal layer over thickness h_1. The contributions to the Moho temperature are:

$$\begin{aligned} \Delta T_0 &= \frac{A_0 h_m^2}{2\lambda} \\ \Delta T_1 &= \frac{\Delta A h_1^2}{2\lambda} \end{aligned} \tag{5}$$

which are such that:

$$\frac{\Delta T_0}{\Delta T_1} = \frac{A_0}{\Delta A} \left(\frac{h_m}{h_1} \right)^2 \tag{6}$$

Typical values for h_m and h_1 are 40 km and 10 km respectively, such that $\Delta T_0/\Delta T_1 \approx 16 \times A_0/\Delta A$. It therefore takes very high values of heat production, higher than the average value for granite (3 μW m^{-3}) for instance, in the upper crust to increase significantly lower crustal temperatures. Even if we use the extreme values from Table 1, $A_0 = 0.2$ and $A_1 = 1.6$, $\Delta A = 1.4$ μW m^{-3}, we find that $\Delta T_0/\Delta T_1 \approx 2$.

3.3. Sensitivity of heat flux and temperature anomalies to the depth of the sources

Models of the temperature and heat flux fields require the specification of the heat production distribution, which is not known. Simple calculations demonstrate that horizontal heat conduction smoothes out lateral changes of heat production and operates as a low-pass filter whose cut-off wavelength increases with source depth (Jaupart, 1983; Nielsen, 1987; Vasseur and Singh, 1986). In this section, we compare the sensitivities of the surface heat flux and the Moho temperature to lateral variations of heat production. We assume that the horizontal distribution of heat production remains the same over some thickness h and that it can be described by elementary periodic functions $f(x,y)$ such that:

$$\nabla_H^2 f(x,y) = \frac{\partial^2 f}{\partial x^2} + \frac{\partial^2 f}{\partial y^2} = -k^2 f \tag{7}$$

where k is the equivalent of a wavenumber. For simplicity, we refer to a single scale or wavelength Δ such that:

$$k = \frac{2\pi}{\Delta} \tag{8}$$

For the sake of example, we set $h = 10$ km in crust of 40 km thickness. Using the results derived in Appendix C, we compare the

variations of surface heat flux and Moho temperature that are induced by such a layer in the upper and lower crust.

For an upper crustal layer, the Moho temperature is much less sensitive to lateral heat production variations than the surface heat flux and, in practice, is not affected by variations at scales that are less than about 100 km (Fig. 3a). Thus, for example, an isolated radioactive granitic pluton of typical dimensions ($\approx$10 km) generates a positive heat flux anomaly at Earth's surface but does not induce any significant temperature rise at the base of the crust.

Results are completely different for heat production in the lower crust, as shown by Fig. 3b. In that case, the Moho temperature and the surface heat flux are equally sensitive to lateral heat production fluctuations. Stated differently, as regards the contribution of lower crustal heat sources, the Moho temperature and the surface heat flux vary on almost identical scales. Another important fact is that variations of heat production in the lower crust at scales that are less than 100 km, if they exist, are not detectable by surface heat flux measurements. Thus, the surface heat flux records a large-scale average of lower crustal heat production.

3.4. Mantle heat flux and lithosphere thickness in the past

These issues are clearly outside the scope of this review but they are worthy of a short discussion. Today's values of the mantle heat flux cannot be calculated from first principles and have been derived from the systematics of heat flow data and (P,T) data in xenoliths from the lithospheric mantle (Appendix B). Constraints on thermal conditions in the Earth's distant past come from essentially two sources, temperatures of basalt mantle sources and lithospheric thicknesses that are required for the stability of Archean diamonds. The former can be used in a well-tested equation for the convective heat flux at the base of a rigid lid, such that the lithosphere is in equilibrium with heat supplied at its base, crustal heat production and heat loss at the surface (Lévy and Jaupart, 2011). For a potential temperature of the Archean mantle that was $\approx$100 K higher than present, the mantle heat flux could have been higher than today by as much as 6 mW m^{-2} (see Fig. 5 in Jaupart et al., 1998). This estimate relies on flow laws for the Earth's mantle which are not tightly constrained (Lévy and Jaupart, 2011), but there is no escaping the fact that the mantle heat flux can only increase if the mantle temperature increases. On the other hand, the thickness of the Archean continental lithosphere has been estimated to be larger than 150 km (Boyd et al., 1985), which does not allow for large changes of the mantle heat flux.

Data from ancient kimberlite eruptions provide information on past lithospheric geotherms. For example, the Gahcho Kue, Grizzly, and Jericho pipes in the Slave Province span a 55–553 My age range but their (P–T) xenolith arrays are identical within measurement error (Canil, 2008), showing that changes of the mantle heat flux are not detectable over that time interval. Similarly, differences between the *ca.* 1.2 My Premier kimberlite xenoliths and much younger, *ca.* 100 My, ones in South Africa are below the resolution limit of current data and thermodynamic methods (Rudnick and Nyblade, 1999). There are differences between the Jericho and Kirkland Lake mantle xenoliths in the Canadian Shield, which have about the same age and lie in different provinces of the Shield, but the slopes of their (P,T) arrays are nearly identical, indicating that the mantle heat flux does not vary laterally (Jaupart and Mareschal, 2015a).

4. Horizontal variations of crustal heat production

4.1. Global data sets

For a statistically homogeneous crust, the total crustal heat production, and thus the surface heat flux, should increase with crustal thickness. One should therefore expect a positive correlation between heat flow and Moho depth, which may be tested by comparing maps of Moho depth and continental heat flow (Figs. 4 and 5). For our present purposes, we exclude the tectonically active regions, where heat flow records transient thermal perturbations and is often higher than 80 mW m^{-2}, and observe that there is no correlation between heat flow and crustal thickness at the global scale (Fig. 6a).

The above analysis is based on imperfect data sets. Moho depths are extracted from the CRUST1.0 model (Laske et al., 2013), which assumes that the crust is stratified in 6 different layers, and gives their average thicknesses within $1^\circ \times 1^\circ$ cells, even where no geophysical data are available. In these geophysically uncharted areas, a crustal column is assigned according to age and tectonic type. The heat flow map, on the other hand, is interpolated between unevenly distributed heat flow measurements on continents (Jaupart and Mareschal, 2011, 2015a). For verification purposes, we have also compiled measurements of both heat flow and crustal thickness at a large number of cells in eastern Canada and confirm the lack of a correlation between heat flow and crustal thickness (Fig. 6b). This implies that the average crustal heat production tends to decrease with increasing crustal thickness, such that $\delta\overline{A}/\overline{A} \approx -\delta h_m/h_m$. One cannot use this to try and estimate heat production from crustal thickness; however, it is an indication that thick crust can only be stable if its bulk heat production is less than average. We return to this point later.

For further interpretation, it would be useful to separate between the contributions of the upper and lower crusts. We find that the power spectrum of the heat flow field is more rugged that that of the crustal thickness due to the strong contribution of the enriched upper crust. A more detailed analysis is not warranted because of the sparsity and uneven distribution of the data.

4.2. The scales of heat production variations

The horizontal scales of heat production variations in the continental crust are not known *a priori* and must be determined from field measurements. Depending on scale, different mechanisms and processes are involved and must be considered separately. Scales of less than about 1 km involve igneous, metamorphic and late alteration processes. For example, one observes that heat production changes across individual horizons in the interior of many plutons, such as the White Mountain batholith, New Hampshire, or the Bohus granite, Sweden (Landstrom et al., 1980; Rogers et al., 1965). At scales of up to a few tens of kilometres, one deals with the dimensions and distances between igneous bodies and metasedimentary formations, with enriched intrusives that may be responsible for very large local heat production anomalies (Table 2). Both types of heat production variations can be assessed easily and do not affect the regional thermal regime, as shown above. Larger scales in a 50–500 km range represent the most difficult challenge. Such scales correspond to the geological fabric of a province over dimensions that are larger than those of individual igneous bodies and are the relevant ones for thermal models of geological interest (Jaupart, 1983; Vasseur and Singh, 1986).

Determining the scales of heat production variations at the surface would require a labour-intensive program of systematic sampling which, to the best of our knowledge, has only been attempted by Eade and Fahrig (1971). These authors collected rocks at the nodes of a periodic grid in the Canadian Shield, but the large number of samples proved to be intractable and powder mixtures were used for chemical analyses. To get around this difficulty, some authors have turned to airborne gamma ray surveys (Andreoli et al., 2006; Bodorkos et al., 2004; Phaneuf and Mareschal, 2014). Using comparisons with a large number of conventional measurements on rock samples in the Sudbury area, Ontario, Phaneuf and Mareschal (2014) have found that the airborne data accurately record differences in heat production from one area to the next, but that they systematically underestimate the true heat production by a factor of >3. The difference can be attributed to alteration and weathering processes that deplete a thin and shallow veneer in Uranium.

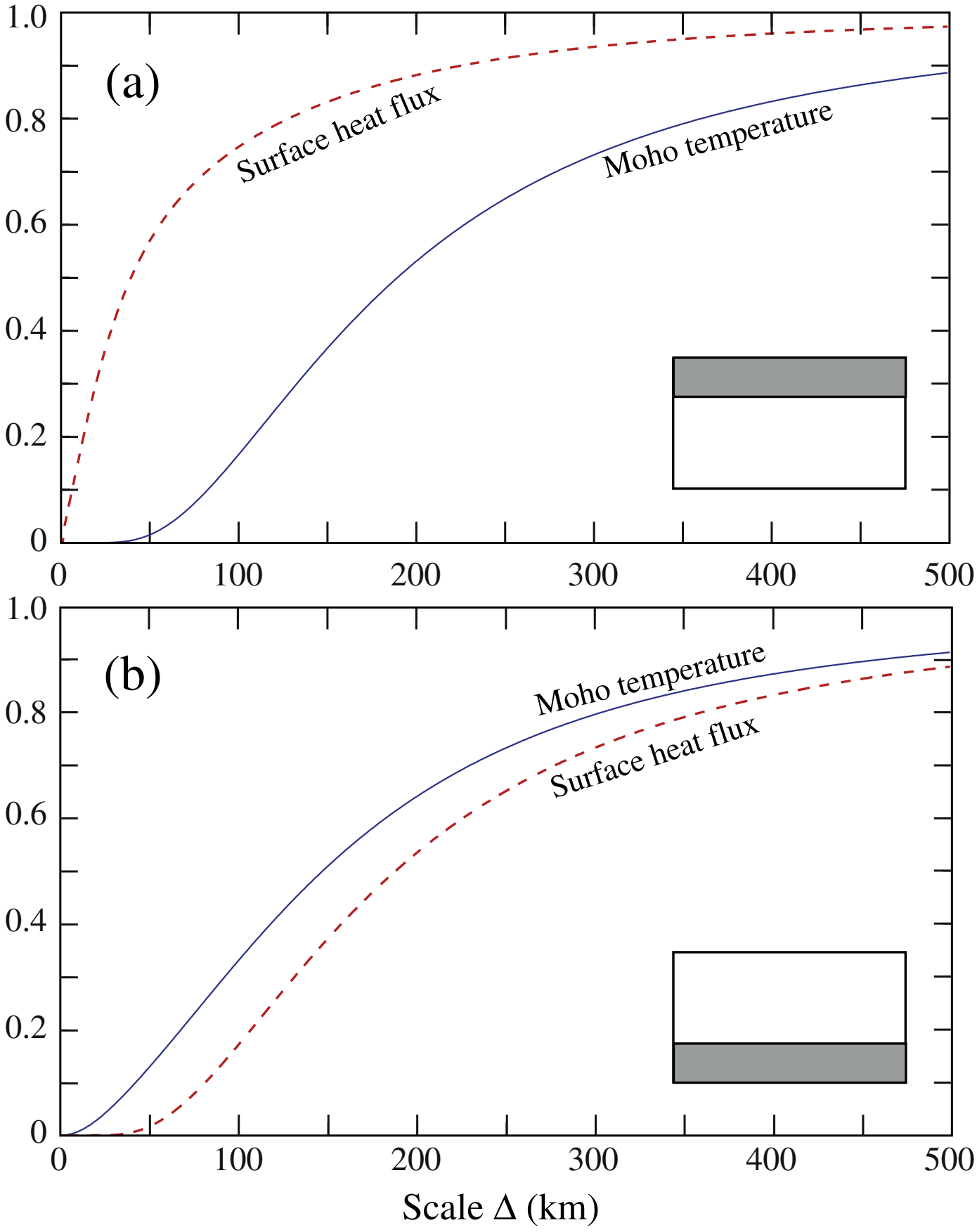
(a)
Surface heat flux
Moho temperature
(b)
Moho temperature
Surface heat flux
1.0
0.8
0.6
0.4
0.2
0
0
100
200
300
400
500
Scale Δ (km)

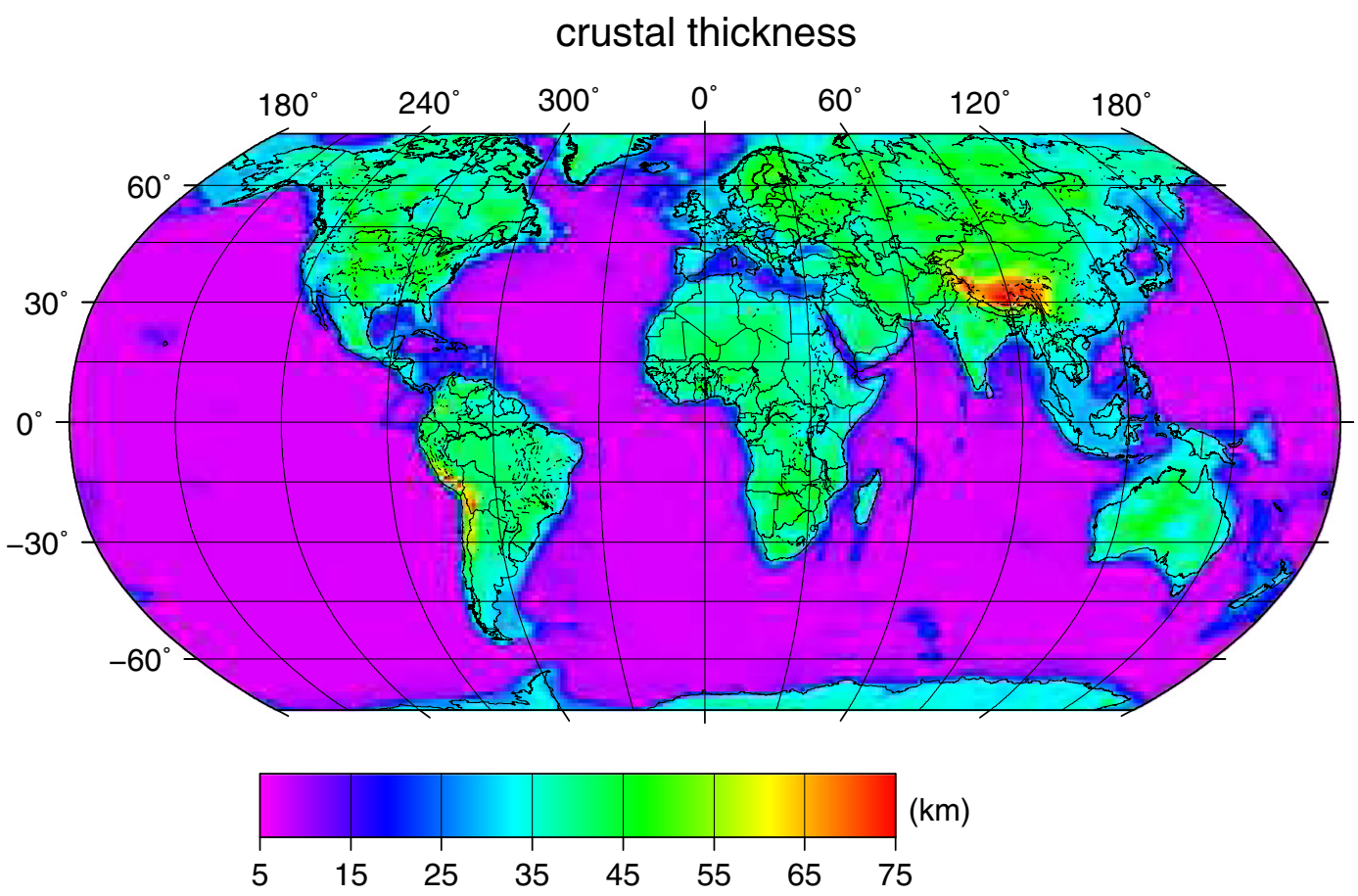

Fig. 4. Map of crustal thickness based on the CRUST1.0 model on a 1° × 1° grid (Laske et al., 2013). For many cells without seismic data, the values for the crustal thickness are based on geological type.

Securing a comprehensive set of evenly distributed heat production measurements in surface rocks seems to be a remote possibility and, even if it was achieved, would not provide information on the lower crust. At present, the only alternative is to use heat flow data. Data are too sparse and unevenly distributed to properly estimate the power spectrum of surface heat flow, but there are enough measurements to assess the scales of heat flow variations in the Precambrian of North America. To this aim, Mareschal and Jaupart (2004) paved the Shield with squares of given dimensions and calculated the average heat flow for each square. They then determined how the mean and standard deviation of these averages vary with the square size, *i.e.* with scale. The mean is almost unaffected by the square size, which shows that the heat flow field is adequately sampled. There is almost no difference between the standard deviation of the individual heat flow values and that of the 50 × 50 km averages (8.9 *vs* 8.8 mW m^{-2}). The standard deviation decreases slightly to 7.3 mW m^{-2} for 250 × 250 km squares and drops markedly to 4.3 mW m^{-2} for 500 × 500 km ones. This analysis shows that most heat flow variations occur over wavelengths that are ≤250 km. As explained above, variations at these scales cannot be due to the mantle heat flux because it originates from the base of the lithosphere. These variations, therefore, can only be generated by crustal heat sources.

4.3. Relationship between heat flow and heat production

Fig. 7a shows that there is no meaningful relationship between the local values of heat flow and heat production in a province. It takes isolated and enriched granitic intrusives, which generate large heat flow anomalies on top of a smoother background, for such a relationship to hold. An affine dependence between heat flow and heat production was found for exceptional sites of this kind by Birch et al. (1968). This remarkable relationship has blinded many authors to the necessity of determining the background heat flow field away from enriched plutons.

In shield areas, surface heat production contrasts tend to be small and heat flux variations are mostly due to changes of basement composition that reflect the geological fabric of a province. This fabric results from the accretion, thrusting and folding of individual belts and older continental fragments. The erosion surface is rarely parallel to the boundaries between individual terranes and cuts across rocks from a range of crustal environments and emplacement depths. One can hope that, over a sufficiently large distance, surface exposures allow a representative sampling of the different rocks that make up the upper crust. If this was true, the average surface heat production would account for a significant volume of upper crustal rocks and would be positively correlated with the heat flux averaged over the same area.

These ideas have been tested in North America by Lévy et al. (2010). They have considered how the relationship between heat flux and heat production depends on horizontal scale. Local values of these two variables are not related to one another, as explained above, and they calculated their average values over two different scales, in geographical windows with dimensions of about 250 km in the interior of several geological provinces of North America and then in the whole provinces, corresponding to a scale of about 500 km. The 250 × 250 km windows

Fig. 3. Amplitude of variations of the surface heat flow and the Moho temperature due to heat production variations in a 10-km thick crustal layer as a function of horizontal scale. Amplitudes are scaled to their values for an infinitely large scale, corresponding to purely vertical heat transport with negligible lateral diffusion. (a) Results for an upper crustal layer. (b) Results for a lower crustal layer located just above the Moho.

are large enough to include enough measurements for the smoothing of small-scale variations and are distributed amongst provinces with contrasting magmatic and tectonic histories. With these windows, a relationship between heat flux and heat production begins to emerge (Fig. 7b). At a larger scale, average values of heat flow and heat production for the five main provinces of North America exhibit a remarkable affine relationship, with a heat flux intercept of ~33 mW m $^{-2}$ for zero surface heat production (Fig. 7c). The 250 × 250 km averages lie close to the province-wide relationship but exhibit greater scatter. Comparing results for the different scales illustrates clearly the difference between heat flow and heat production. In the Grenville province, for example, the 250 × 250 km and province-wide averages are (39mW m^{-2}, 0.47 μW m^{-3}) and (41 mW m^{-2}, 0.80 μW m^{-3}), respectively. The heat flux is barely affected by the change of scale, whereas the heat production almost doubles.

The remarkable relationship between the province-wide values of heat flow and heat production (Fig. 7c) is difficult to reconcile with significant variations of the Moho heat flux beneath North America. This relationship requires that, if such variations do exist, they get cancelled by opposite variations of lower crustal heat production. It is impossible to find a physical explanation for such a strong link between two completely independent variables and the most sensible hypothesis is that the Moho heat flux is approximately the same beneath the five provinces. Variations of the Moho heat flux may not be exactly zero but must be smaller than departures from the best-fitting relationship, or about 2 mW m^{-2}, which is close to the intrinsic uncertainty of heat flow measurements (Mareschal and Jaupart, 2004). Such potential variations are small compared to those of the surface heat flux but represent a significant fraction of the average Moho heat flux of 15 mW m^{-2}. As shown by Lévy et al. (2010), they may be associated with variations in lithospheric thickness up to 30 km.

It would be desirable to carry out the same analysis in other continents but no data set of comparable size seems to be available, due mostly to incomplete heat production coverage. It is useful, however, to adopt a similar approach wherever possible and this is done for two continental regions in the next section.

4.4. Regional studies

4.4.1. Norwegian shield

The heat flow field of Fennoscandia is now well documented (Fig. 8) and shows a marked contrast between the western regions and the generally older shield that lies to the east. Heat production measurements have been made in large quantities in Norway over different types of crust, including part of an Archean province, several Proterozoic belts and the recent Oslo rift. Heat flow and heat production values at individual sites are not correlated with one another: heat production may vary by as much as a factor of 3 for sites with the same surface heat flow (Slagstad et al., 2009). Recognizing that heat flow records heat production over a larger volume than the immediate neighbourhood of a measurement site, Slagstad et al. (2009) have determined the average heat production of rocks within a 10 km radius and found no correlation with heat flow. This shows that the crust is highly heterogeneous on a 10 km scale in both the horizontal and vertical directions, at least from the standpoint of heat production. Averaging measurements within each geological sub-province, however, one finds a stronger relationship between heat flow and heat production (Fig. 9). The data do not conform to an affine relationship, indicating that the sub-

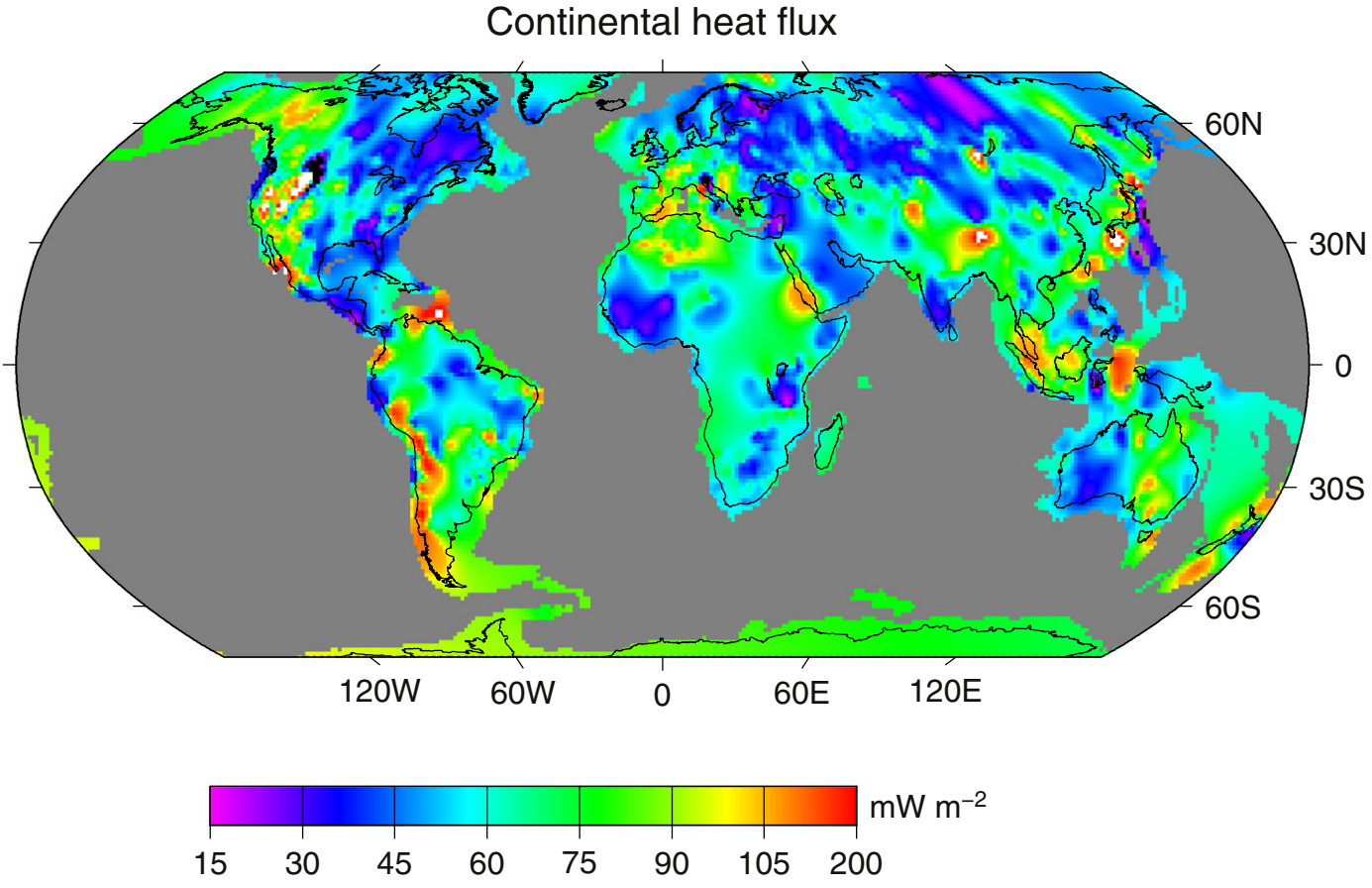

Fig. 5. Map of continental heat flux based on ≈35,000 unevenly distributed continental heat flow measurements. For tectonic active regions, the heat flow is not in steady state and includes a transient perturbation on top of crustal heat production; in tectonically stable regions with a steady state thermal regime, variations in surface heat flux directly reflect variations in crustal heat production. Note the higher variability of the heat flux compared with crustal thickness.

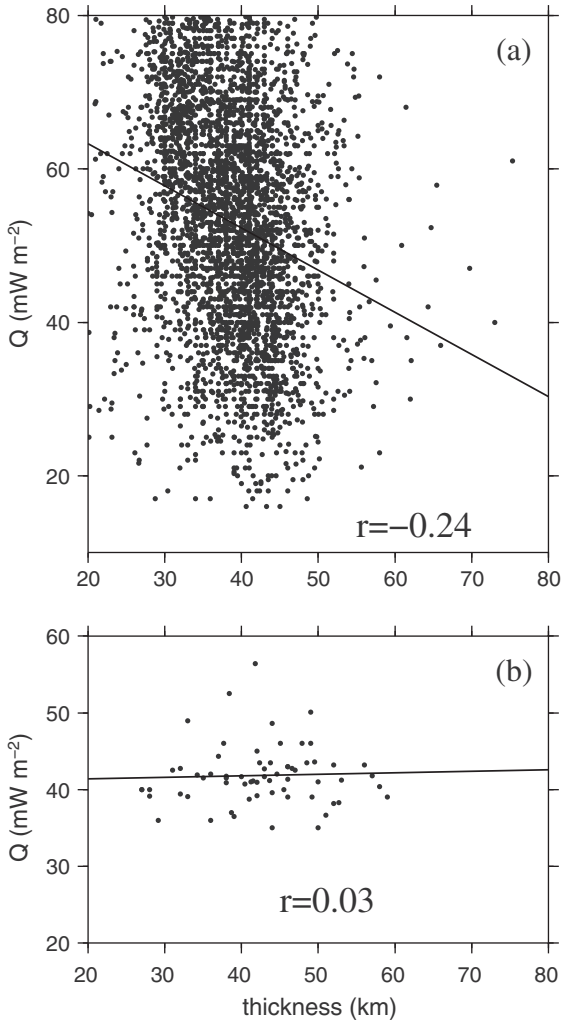

Fig. 6. Scatter plot of heat flux and crustal thickness. (a) Global data set comparing heat flux averaged over 1° × 1° cells *vs* crustal thickness from CRUST1.0. The solid line represents the best linear "fit" to the cloud of points (with a correlation coefficient r = −0.24). (b) Data from eastern Canada. Heat flux data have been averaged over 1° × 1° cells and their values are plotted against the corresponding crustal thickness values from Lithoprobe (Perry et al., 2002) and recent receiver function studies (Fiona Darbyshire, pers. comm.). The plot shows no trend and the correlation coefficient between the two data sets r = 0.03.

provinces have different upper crustal structures. Large changes of heat flow occur over small lateral distances, which confirms that they are generated in the upper crust.

4.4.2. United Kingdom

Data from the United Kingdom provide an interesting counterexample. There, the crystalline basement is made of three large granitic batholiths that surround the late Proterozoic and Phanerozoic gneisses and metasedimentary rocks of central England and Wales. The batholiths, that extend over lateral distances at least 100 km in all directions, represent significant portions of continental crust. The three batholiths and the central region show up as well-separated fields in a heat flow *versus* heat production diagram (Fig. 10). Taken as a whole, the UK data set suggests a very rough trend of increasing heat flow with increasing heat production but does not show any meaningful relationship between the two variables, with heat flow that may vary by a factor more than 2 at a constant value of heat production. Compared to the small heat flux values of central England and Wales, the elevated ones on batholiths can be accounted for by heat production contrasts over thicknesses that differ markedly between the three batholiths.

Table 2
High heat production granites.

Name	Heat production (μWm^{-3})			Reference
	Average	Min	Max	
Archean				
Cartier Batholith (Superior, Can)	4			Meldrum et al. (1997)
Lac de Gras (Slave, Can)	8.1	4.9	15.9	Thompson et al. (1995)
	6.4	5.3	8.1	Thompson et al. (1995)
Bundelkhand craton (India)		4.0	4.8	Kumar et al. (2009)
Proterozoic				
Bohus (Norway)	6.4			Landstrom et al. (1980)
Eastern Gawler Craton (Aus)	7.5	3.4	17.0	Neumann et al. (2000)
Namaqua complex (South Af.)	3.7	0.86	46.0	Andreoli et al. (2006)
Chotanagpur gneiss complex (India)		3.9	6.5	Kumar et al. (2009)
Phanerozoic				
Mount Painter Province (Aus)	16.1	4.5	60.1	McLaren et al. (2006)
S W England batholith	4.7			Tammemagi and Smith (1975)
White Mountains (App, USA)	8.5			Roy et al. (1968)

5. Large-scale controls on the bulk crustal heat production

The above overview has established a few important points. Geological provinces and sub-provinces can be identified and separated from one another according to their respective average values of heat flow and heat production. With only one of these two variables, such separation would not be possible. Heat flow differences are largely due to changes in the composition of the crust, and variations of the Moho heat flux are near the resolution threshold of the data.

5.1. Significance of average crustal characteristics

The need to work with averaged values of heat flux and heat production puts us at a disadvantage. At the large scale that is required, the averaging procedure lumps together a variety of terranes and tectonic features, so that the end result may not reflect the geological processes that have shaped a province. To check that the average values of heat flow and heat production are truly representative of the crust of a province, one can divide the province in different sub-provinces and compare their thermal characteristics. This also allows a test of the repeatability of crust forming mechanisms. There are enough measurements for such an analysis in the Superior province and the Appalachians (Table 3). In the former province, data are available for three different volcanic belts whose accretion to an older core marked the end of the craton assembly process at 2.7 Gy. Their average values of heat flow and heat production are remarkably close to one another, testifying to a tight control on the composition of juvenile crust at that time. The Appalachians province, which stretches over a large distance along the eastern edge of North America, can be split arbitrarily into its US and Canadian parts. Heat flow and heat production data for these two parts are statistically identical (Table 3), which shows that the characteristics of the Appalachian crust do not vary significantly along strike.

5.2. Large-scale pattern

Nyblade and Pollack (1993) had noted a rather systematic pattern of low heat flow in Archean cratons and higher heat flow in adjacent Proterozoic terranes, which they attributed to change in mantle heat flux.

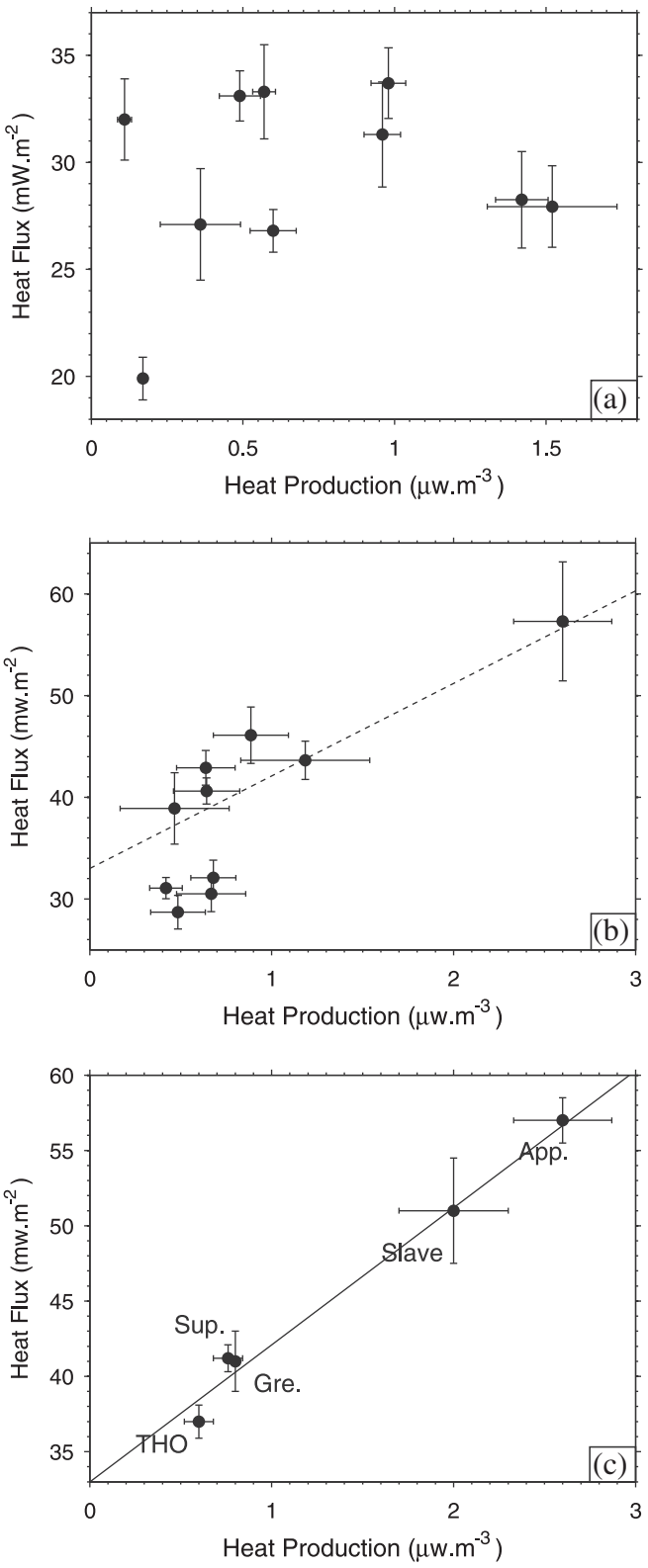

Fig. 7. Plot of surface heat flow as a function of surface heat production for three different scales in the Canadian Shield and the Appalachians, from Lévy et al. (2010). (a) Local values in the northern part of the Superior province, Canada. (b) Average values for ten 250×250 km windows with a large number of measurements. The dashed line is the best-fit linear relationship to values at the largest scale. (c) Average values for the five main geological provinces of North America, the Archean Slave and Superior provinces, the Proterozoic Trans-Hudson Orogen (THO) and Grenville provinces and the Phanerozoic Appalachians province.

In light of the new data that have been collected, this observation and their conclusions should be qualified. In the Superior Province, the core of the craton is characterized by low heat flow and is surrounded by younger accreted belts with higher heat flow (Jaupart et al., 2014), but these belts are also Archean, so that the difference has nothing to do with age. One can attribute such heat flux contrasts to three causes: (1) a long-term transient reflecting the slow thermal relaxation that follows continent formation, (2) differences of crustal heat production and (3) differences of heat supply to the base of the lithosphere (the mantle heat flux). The transient effect has been convincingly rejected by Nyblade and Pollack (1993) using both observations and simple theoretical arguments which need not be repeated here. In all cases that are known to us, it may be shown that the heat flux contrast between craton core and surrounding belts is in large part due to a change of crustal heat production. One observation is simply that the heat flux contrast is associated with one of heat production. In addition, the change of surface heat flux occurs abruptly at the craton edge over a distance that is less than the crustal thickness, showing that it has a shallow origin. This is observed at the boundary between the Archean Kaapvaal craton and the Proterozoic Namaqua-Natal belt in Lesotho, for example (Jones, 1992). Where there is no contrast in crustal heat production, such as between the Archean Superior province and the Trans-Hudson orogen or the Grenville province, there is no difference in heat flux (Jaupart and Mareschal, 1999).

Variations of heat flux at the base of the lithosphere, if they exist, can only affect the surface heat flux over very large horizontal scales (>≈500 km), as shown above. Because of this, they are difficult to detect with surface measurements. In fact, they are not required by the data and it may be worth pointing out that, within a continent, variations of lithosphere thickness do not necessarily require variations of the mantle heat flux. By analogy with the oceans, there has been a tendency to link surface heat flux to lithosphere thickness, such that an elevated heat flow implies a thinner lithosphere. With the large values of heat production that characterize continental crust, this interpretative framework is not valid. Large variations of the mantle heat flux are ruled out by the parallel (P,T) arrays of lithospheric xenolith suites from different parts of Canada and South Africa (Jaupart and Mareschal, 2015a). Horizontal changes of crustal heat production are large enough to induce significant variations of Moho temperature and lithosphere thickness by themselves.

5.3. Variations of crustal heat production with age

Using global heat flow data sets, several authors have proposed that continental heat flow decreases with age, which can be attributed to the thermal relaxation of an early lithospheric thermal event or to a decrease of crustal heat production. This ambiguity cannot be resolved without a joint analysis of heat flow and heat production data. The apparent variation of heat flow with age is essentially due to the large difference that exists between tectonically active regions and Archean provinces. Morgan (1985) pointed out that, if one excludes these two extremes, the differences in heat flow between age groups are not statistically significant. He further noted that the low heat flow of Archean provinces is associated with low values of heat production. Using a large data base of heat flow and heat production data, Jaupart and Mareschal (2014) found that there is indeed a trend in the distribution of crustal heat production with age (Table 4, Fig. 11). One must beware, however, that there is a very wide range of crustal heat production within each age group. Extremely high values of heat production (>5 μW m^{-3}) have been measured on granitic plutons and gneisses of all ages and provenances, including Archean ones (Table 2). When corrected for the rundown of the radioactive elements, heat production values in some Archean granites and gneisses are comparable to, and in some cases greater than, that of the young and markedly enriched Appalachian White Mountain pluton. Very high values of heat production have also been found in several Proterozoic provinces, including the

entire Gawler craton, central Australia (McLaren et al., 2003; Neumann et al., 2000), or the Wopmay orogen in northwestern Canada (Lewis et al., 2003).

Accounting for the rundown of heat producing elements due to radioactive decay, we find little change in the value of heat production at the time of crustal stabilization (Fig. 11), suggesting that the thermal conditions for stabilization have not varied significantly. Table 5 lists data for four well-documented provinces spanning a large age range. These four provinces have been affected by high-temperature metamorphism, indicating that crustal temperatures have not changed markedly through geological time. At present, the crustal heat flow component is smaller in the Archean province than in the younger ones but, once it is corrected for age, it is as large as in these provinces.

6. Vertical distribution of heat producing elements

It was understood very early that heat production must decrease with depth in the Earth's crust because otherwise, with the heat production rates of surface rocks, the crustal heat flow component would exceed the surface heat flux (Birch et al., 1968; Jeffreys, 1936). The geochemical models of Table 1 illustrate this but allow a large range of values for the lower crust. This is due in part to the non-uniqueness of the relationship between seismic velocities and composition and in part to the different crust-building processes that may be active in island arcs. Hacker et al. (2011) have argued that felsic gneisses may be "relaminated" to the base of the crust, leading to lower crust that is less depleted than commonly thought. Given the number of accretion mechanisms and tectonic events that shape the continental crust, one can hardly advocate a single universal model for the vertical distribution of heat production. One must again devise methods that may be implemented locally and there is at present no alternative to the use of heat flow data. A major difficulty is that upper crustal heat sources are responsible for a significant part of the surface heat flux but have a small impact on deep crustal temperatures, as explained above. Thus, it is essential to determine the part of the surface heat flux that is not generated in the upper crust, which will be noted q_r. In steady-state, this heat flux component is the sum of the Moho heat flux and heat released in the mid and lower crusts.

6.1. Determining the upper crustal heat flow component

In order to determine the heat flux at the base of the upper crust, which has been called the "reduced" heat flux, an obvious method is to find areas where the upper crust has zero or negligible heat production. This is rarely possible and an alternative method is to seek a relationship between heat flux and heat production that can be extrapolated to zero heat production. In a few cases, the data conform to an affine function of the form:

$$q_o = q_r + DA_S \tag{9}$$

where q_o and A_S are the surface values of heat flow and heat production at individual sites. This simple relationship allowed excellent fits to measurements that were available to Roy et al. (1968) in a few North American provinces. In the simplest interpretation, the intercept q_r is the heat flux at the base of an upper crustal layer of thickness D. It is now recognized that this relationship is not valid in many geological provinces, as discussed above and demonstrated by Figs. 7a and 10. It is still used by many authors for a least-squares fit through heat flux and heat production data.

In the early days of heat flow studies, there were very few "heat flow provinces" where enough data were available for an analysis of heat flux and heat production. For those provinces, measurements were biased in favour of enriched intrusives and turned out to be approximately consistent with an affine relationship. Pollack and Chapman (1977) derived values of the average surface heat flux and reduced heat flux and found that $q_r \approx 0.6\overline{q_o}$. They noted that the slopes of the heat flow heat production lines are all of the order 10 km and proposed that it represents the near constant thickness of the enriched upper crustal layer. Assuming that the heat production is 0.25 μW m^{-3} throughout the middle and lower crusts, they came up with estimates of the mantle heat flux even in areas with no heat production data, and derived characteristic continental geotherms that depend only on the surface heat flux. With this approach, values of the surface and mantle heat flux must vary in tandem. Temperature variations at the base of the crust are larger than in models where differences in heat flux come mostly from crustal heat production.

In a more recent world-wide compilation, Artemieva and Mooney (2001) have used the affine relationship to derive values of q_r and D in a large number of provinces. In many cases, the data are clearly not consistent with such a relationship and the method was adopted for want of an alternative one. Artemieva and Mooney (2001) assumed that heat production decreases exponentially with depth, as $\exp(-z/D)$, and that, below a depth that was set equal to D, heat production remains constant in the mid and lower crustal layers (with values of 0.4 and 0.1 μW m^{-3} respectively). Values of D, where they can be estimated, seem to lie in a restricted range around a mean value of 10 km. In this framework, the heat production of the mid and lower crust is almost constant if one excludes variations in crustal thickness, so that variations in the Moho temperature arise mostly from changes of mantle heat flux.

Acknowledging the limitations of a best-fit procedure through highly scattered heat flux and heat production data, Hasterok and Chapman (2011) have proposed a new approach. They postulated that q_r is proportional to the surface heat flux, such that $q_r = \beta\overline{q_o}$, where β is a constant to be found. For a prescribed value of 0.4 μW m^{-3} for heat production in the mid and lower crusts, they calculated lithospheric geotherms for different values of the surface heat flux and a fixed β. Additional constraints were required to determine the value for β. Hasterok and Chapman (2011) calculated elevation in the isostatic limit for several geological provinces and obtained the best agreement with the observations for $\beta = 0.74$. With such a large value, variations of the surface heat flux are transferred to the reduced heat flux with little change and, with the low value of crustal heat production that is postulated for the mid and lower crusts, to the Moho heat flux also. This allows for large variations of the mantle heat flux, which induce the deep seated differences in lithospheric temperature and density that are required for thermal isostasy. Such calculations rest on the assumption of thermal steady state, however, which is not verified for the active tectonic regions with the highest heat flow (>75 mW m^{-2}) and "compositionally adjusted" elevation values. Hyndman (2010) showed that the elevation and crustal thickness data follow two distinct trends, one for stable and one for active regions. With the method of Hasterok and Chapman (2011), geotherms are slightly higher and the range of mantle heat flux values is wider than that obtained by Artemieva and Mooney (2001).

6.2. Sampling the mid and lower crusts

The above methods require values for heat production beneath the upper crust, which cannot be measured directly. One has to turn to rocks that have been exposed to deep crustal conditions and that are available as xenoliths in kimberlites (Rudnick and Taylor, 1987), in terranes that have been brought to the surface along thrust faults (Fountain and Salisbury, 1981) or, exceptionally, by rebound of the crust following a large meteorite impact (Nicolaysen et al., 1981). Hasterok and Chapman (2011) have compiled data from 31 granulite facies terranes throughout the world and found a very wide spread of heat production with a mean of 0.68 ± 0.62 μW m^{-3} (mean and standard deviation).

Granulite facies metamorphism can occur over a rather large pressure range and is not necessarily representative of lower crustal conditions. Table 6 lists measurements for 18 terranes sorted by age and

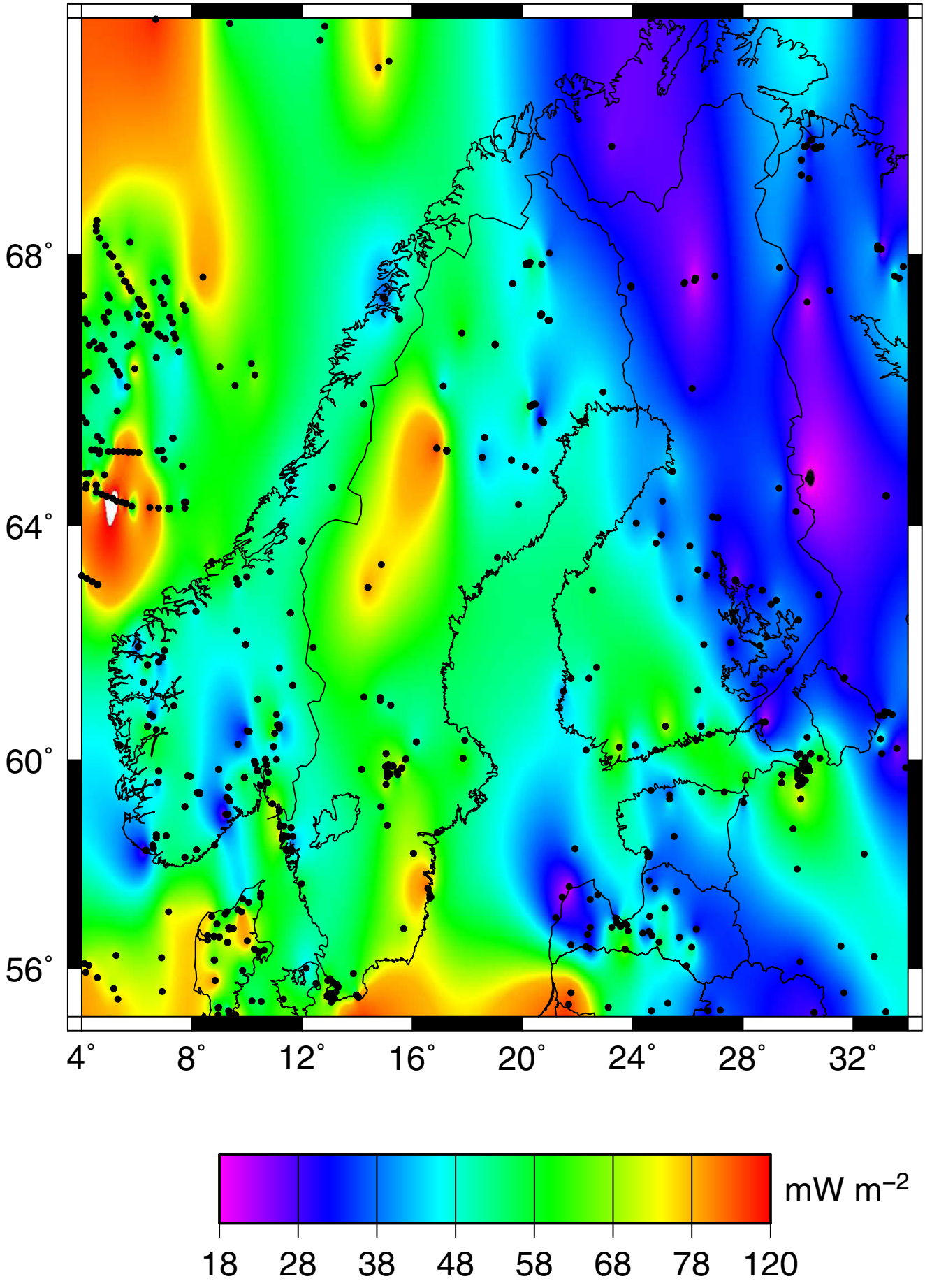
68°
64°
60°
56°
4°
8°
12°
16°
20°
24°
28°
32°
mW m−2
18
28
38
48
58
68
78
120

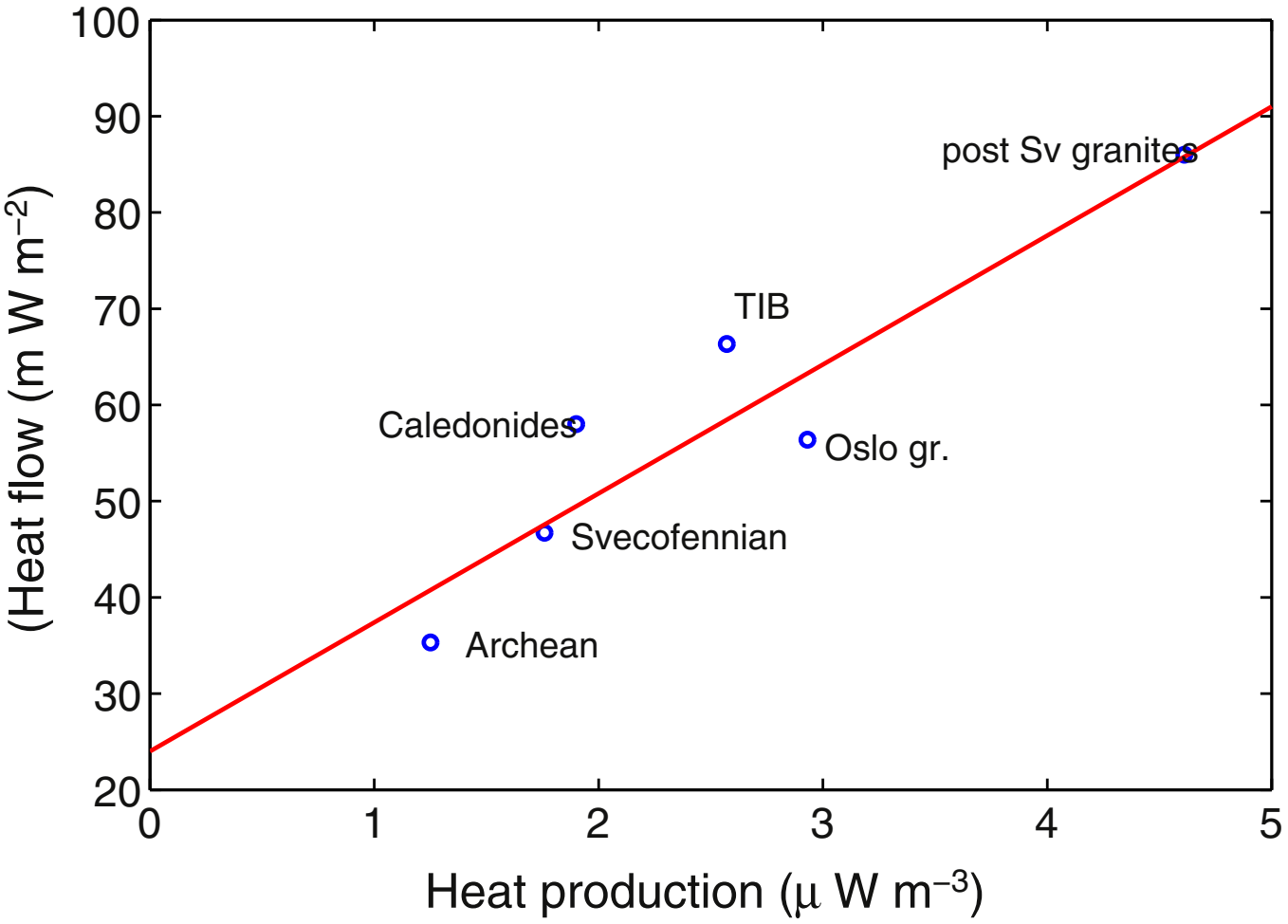

Fig. 9. Relationship between heat flow and heat production in Fennoscandinavia, from Slagstad (2008). The data are averaged over 6 regions according to location and geological type. The best fitting line is $\bar{Q} = 24.5 + 13.4\bar{A}$. TIB is the TransScandinavian igneous belt.

metamorphic pressure conditions. A rigorous statistical analysis is not warranted for such a limited data set but one can note a definite trend of decreasing heat production with increasing metamorphic pressure. There seems to be no significant variation as a function of age. The lowest values are found in Archean terranes but they fall within the range of values for younger provinces once they are corrected for radioactive decay.

This brief overview shows that heat production in the mid to lower crusts is not negligible and can be much higher than the global estimates of Table 1. It varies by large amounts between provinces and may be responsible for significant heat flow variations.

6.3. Assessing the extent of crustal stratification

We have described several attempts to deduce the crustal heat flow component and, by way of consequence, the mantle heat flux from heat flux and heat production data. An alternative approach relies on estimates of the mantle heat flux, which has the advantage of imposing no *a priori* constraints on crustal stratification. On the contrary, this method aims at estimating the degree of crustal stratification (Perry et al., 2006a).

If the mantle heat flux q_m and the crustal thickness h_m can be determined independently, one can estimate the bulk average heat production of the crust, noted $\overline{A}_c$, as follows:

$$\overline{A}_c = \frac{\overline{q_o} - q_m}{h_m} \tag{10}$$

From knowledge of the average value of heat production in surface rocks, A_S, one can calculate a "differentiation index" (Perry et al., 2006a):

$$DI = \frac{A_S}{\bar{A}} = \frac{A_S \times h_m}{\bar{q}_o - q_m} \tag{11}$$

DI is equal to 1 if the crust is not stratified and is larger than 1 in many geological provinces because the upper crust is enriched compared to the bulk. This does not specify the thickness *h* of the superficial layer, which must be less than the crustal thickness h_m. If $DI > 1$, an upper bound for *h* is obtained by assuming that the lower crustal heat production is negligible, such that $h = h_m/DI$. Estimates for *h* can be obtained by fixing heat production in the deeper crust, or can be deduced from a regional heat flow heat production relationship. Uncertainties on these

Fig. 8. Heat flow map of Fennoscandia, from data in Slagstad et al. (2009). Heat flow decreases markedly towards the Archean Baltic Shield to the East. Several intermediate-scale (≈120 km) heat flow anomalies are generated by enriched or depleted rocks.

estimates are difficult to assess but it may be shown that, for given values of DI and $q_c = \overline{q_o} - q_m$, their impact on temperature calculations is small.

The large-scale bulk thermal characteristics of the crust in a number of geological provinces are listed in Table 7. DI values are spread over a wide range, indicating a variety of crustal structures. The differentiation index is about 1 in several cases. In the Canadian part of the Grenville province, this is due to the small average value of surface heat production, which is itself a consequence of the many depleted anorthosite bodies that are present in the upper crust. In some greenstone belts, such as the Abitibi or the Flin Flon Snow Lake belt of the Trans-Hudson orogen, Canada, $DI<1$ because the uppermost crust is made up of mafic volcanics that have been transported over a more radioactive basement. In the case of the Trans Hudson orogen, this basement has been recognized as the Archean Sask craton (Hajnal et al., 2005).

If an upper crustal layer is enriched by a factor DI with respect to the mean crust, the crustal component to the Moho temperature is obtained as:

$$\Delta T_c = (q_0 - q_m)\frac{h_m}{2\lambda}\left[1 + \frac{h}{h_m}(1 - DI)\right] \quad (12)$$

where h is the thickness of the enriched layer. One can see that the Moho temperature decreases with increasing DI value, *i.e.* with increasing enrichment of the upper crustal layer.

7. Thermal control on crustal thickness

The thickness of continental crust varies but in a relatively narrow range (Fig. 12). This range would be even narrower if tectonically active regions were excluded. One should also note that there are very few regions where the crust is thicker than 60 km. These observations raise two independent questions: what controls the average thickness of ≈38 km, and how can the crustal thickness be constrained to lie within a small range.

We address these questions with arguments on the thermal structure of the crust. Our calculations rest on the assumption of thermal steady state which is, obviously, not valid at the time of crustal stabilization or during an orogenic event. Transient calculations require assumptions on the mechanism of crust formation as well as on the rates of tectonic deformation/accretion, which are outside the scope of this paper. They are very sensitive to heat production, however, and deviate markedly from steady-state predictions only in early phases of activity (England and Thompson, 1984; Gaudemer et al., 1988; Huerta et al., 1998; Mareschal and Jaupart, 2006; Michaut et al., 2009). Deformation and magmatic activity develop in belts of finite width, so that one should in principle account for lateral heat transport and across-strike variations of thermal structure. Nervertheless, axial regions are effectively close to one-dimensional conditions in belts that are wider than about 250 km (Gaudemer et al., 1988).

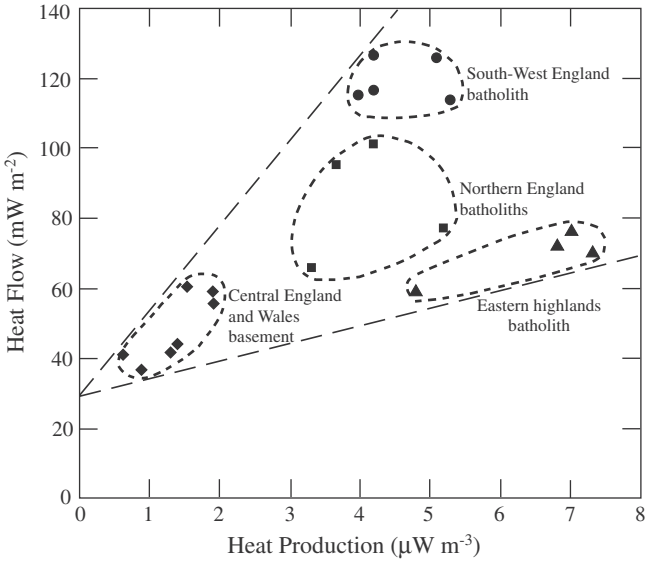

Fig. 10. Relationship between heat flow and heat production in the United Kingdom, from Webb et al. (1987). The data are grouped in four domains according to location and geological type (short-dashed outlines). The two long-dashed lines have slopes of about 5 and 24 km, and indicate the thicknesses of enriched rocks that are required to account for the heat flow variations between the different domains.

Table 3
Mean heat flow and surface heat production in different parts of the same geological province. The mean heat production is that of all the samples from the heat flow sites.

	Heat flow (±σ) (mW m^{-2})	Heat production (±σ) (μW m^{-3})	Reference
Accreted Terranes, Superior Province, Canada			
Wabigoon	42.5 ± 7.3	0.66 ± 0.51	(1)
Wawa	44.4 ± 8.0	0.85 ± 0.40	(1)
Abitibi (west of 77°W)	43.3 ± 7.0	0.59 ± 0.52	(1)
Appalachians			
Canada part	56 ± 12	2.6 ± 2.0	(2)
U.S. part	58 ± 13	2.5 ± 1.9	(2)

References: (1) Jaupart et al. (2014), (2) Mareschal et al. (2000a).

7.1. Melting and intracrustal fractionation

For given values of the differentiation index, the surface and the mantle heat flux, one can calculate the Moho temperature. Fig. 13 gives results for the present average heat production of Archean crust of 0.7 μW m^{-3}, corresponding to 1.5 μW m^{-3} at the time of crustal stabilization, which we take to be 2.7 Ga. At that time, the crustal temperature component ΔT_c was twice present, *i.e.* ≈600 K. Accounting for the Moho heat flux, that we assume to be at least as large as today (≈15 mW m^{-2}), adds another 300 K to Moho temperature. In steady state conditions, the base of a 40 km thick undifferentiated crust, was thus at ≈830 °C, near melting. This has been known for a long time and led Morgan (1985) to propose that only Archean crust depleted in heat producing elements could have remained stable and survived. One alternative solution to stabilize the crust, however, is to concentrate the heat sources in an enriched upper layer, which lowers temperature. As shown in Fig. 13, this is a major effect.

Independently of the degree of intra-crustal differentiation, the Moho temperature remains elevated when the crust thickens. For a 50 km deep Moho, it exceeds the implausible value of 1500 °C for homogeneous crust and remains >900 °C for highly differentiated crust (Fig. 13). It is therefore clear that crustal heat production imposes an upper limit on crustal thickness in Archean time. The same argument applies to recent provinces with similar values of the crustal heat flow component.

Table 4
Average crustal heat production range A and crustal heat flow component q_c calculated for a 40 km thick crust *vs* crustal age group.
From Jaupart and Mareschal (2014).

Age group	A (μW m^{-3})	q_c (mW m^{-2})	% area[a]
Archean	0.56–0.73	23–30	9
Proterozoic	0.73–0.90	30–36	56
Phanerozoic	0.95–1.21	38–48	35
Total continents	0.79–0.99	32–40	

[a] Fraction of total continental surface, from model 2 in Rudnick and Fountain (1995).

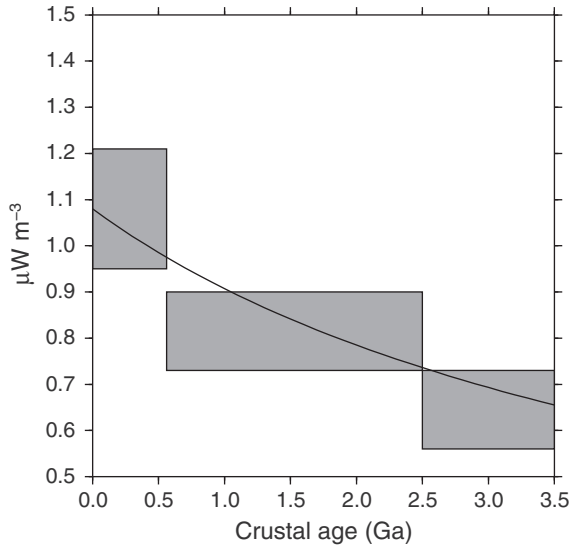

Fig. 11. Average crustal heat production as a function of age, from Jaupart and Mareschal (2014). The large width of the age groups is due to the large spread of heat production values at any given age, which does not allow a fine scale separation. The thick curve illustrates the rundown of heat producing elements due to radioactive decay. After correction for this rundown, the crustal heat production at the time of crustal stabilization is essentially constant.

These temperature estimates also bear on the fate of mafic and ultramafic cumulates that are by-products of the generation of silicic continental material in volcanic arcs or plateaux. The bulk composition of continental crust can only be explained if these rocks are removed, which requires them to be denser than the underlying mantle. At pressures in a 0.8–1.1 GPa range, corresponding to the average continental Moho depth, this requires in turn that temperature is less than about 800 °C (Jull and Kelemen, 2001). At pressures less than 0.8 GPa, most mafic lithologies are stable regardless of temperature. Thus, thin crust cannot release mafic cumulates and evolve towards the bulk felsic compositions that are observed. One can envision gradual thickening of a proto-crust made of both felsic rocks and mafic residues until a minimum pressure of about 0.8 GPa (a minimum thickness of about 30 km) is reached. Further additions to this crust, which does not have high heat production, would stay at temperatures lower than 800° and lose their mafic residues, thereby enhancing heat production of the leftover material. Felsic crust could grow in this manner up to a thickness of about 40 km. At this point, without intracrustal fractionation, Moho temperatures become too high for mafic cumulates to be denser than the mantle and this mechanism would no longer work. This conceptual sketch shows that the interplay between density, temperature and pressure, which is critical to the accumulation of felsic crustal material, cannot be studied without attention to heat production. In short, it is the pressure control on density that allows mafic crust to founder whereas it is the heat production control on temperature that prevents felsic crust from becoming too thick.

Table 6
Heat production of granulite facies terranes in different regions ranked by age and maximum pressure of granulite facies metamorphism.

Location	Age	Pressure	Heat production	Reference
	(Gy)	(GPa)	(μW m^{-3})	
Archean				
Vredefort (South Africa)	>3.1	0.4–0.6	1.0	(1)
Western Dharwar craton (India)	2.7	0.5–0.7	0.65	(2)
Western Dharwar craton (India)	2.7	0.7–1.1	0.35	(2)
Eastern Dharwar craton (India)	2.7	0.5–0.7	0.35	(2)
Eastern Dharwar craton (India)	2.7	0.7–1.1	0.16	(2)
Kapuskasing (Superior, Canada)	2.65	1.0–1.1	0.40	(7)
Pikwitonei (Superior, Canada)[a]	2.6	0.6–1.1[†]	0.40	(3)
Varpaisjarvi (Finland)	2.6	0.8–1.1	0.57	(4)
Scourie (NW Scotland)	2.7	0.85–1.15	0.11	(5)
Proterozoic				
Turku (Finland)	1.82	0.4–0.6	2.24	(4)
Egersund (Norway)	1.0	0.4–0.6	0.40	(6)
Pielavesi (Finland)	1.89	0.45–0.65	0.96	(4)
Southern Estonia	1.83	0.6	1.35	(4)
Lapland (Finland)	2.0	0.6–0.7	1.0	(4)
Eastern Ghats (India)	1.0	0.8–1.2	0.26	(8)
Musgrave Range (Australia)	1.2	1.2	0.30	(9)
Phanerozoic				
Ivrea Zone (Italy)	0.3	0.6–0.9	0.40[b]	(10)
South Altay belt, NW China	0.35–0.30	0.91–0.93	0.97	(11)
Global dataset				
Terranes worldwide	/	/	0.68 ± 0.62	(12)

References: (1) Nicolaysen et al. (1981); (2) Kumar and Reddy (2004); (3) Fountain et al. (1987); (4) Joeleht and Kukkonen (1998); (5) Rollinson (2012); (6) Pinet and Jaupart (1987); (7) Ashwal et al. (1987); (8) Kumar et al. (2007); (9) Lambert and Heier (1967); (10) Galson (1983); (11) Yang et al. (2015); (12) Hasterok and Chapman (2011).
[a] Samples from several parts of the Pikwitonei with different metamorphic pressures.
[b] Heat production value for a mixture of felsic and mafic lithologies (metapelites and stronalites on the one hand and a mafic complex on the other hand).

7.2. Tectonic crustal thickening

In compressional regime, the crust can be thickened by uniform shortening or by thrusting. Both mechanisms increase the total crustal heat production in proportion to the amount of thickening. The thermal consequences can be laid out very simply for a homogeneous crust. Defining the thickening $\phi = \delta h_m / h_m$ and assuming that the Moho heat flux is unchanged, the crust and mantle contribution to Moho temperature vary as follow:

$$\Delta T_c = \frac{A(h_m + \delta h_m)^2}{2\lambda} = \frac{A h_m^2}{2\lambda} \times (1+\phi)^2$$
$$\Delta T_m = \frac{q_m(h_m + \delta h_m)}{\lambda} = \frac{q_m h_m}{\lambda} \times (1+\phi) \quad (13)$$

Doubling the crustal thickness multiplies the mantle component of Moho temperature by a factor 2 and the crustal component by 4. Referring to Section 3.1, the mantle and crustal contributions to Moho temperature are about 300 K each. Thickening the crust by a factor 2

Table 5
Crustal component of heat flow in high-T metamorphism provinces. Average surface heat flux, $\overline{q_o}$, mantle heat flux, q_m, crustal component, q_c.

Province	Age	T,P conditions	$\overline{q_o}$	q_m	q_c	q_c (past)[a]	Reference
	(Gy)	(°C, GPa)		mW m^{-2}			
Superior, Can. (accreted belts)	2.7	725–810, 0.6–0.7	44	15	29	61	(1)
Namaqua, S. Africa	1.05	800–1000, 0.6–0.8	61	18	43	54	(2)
Mount Painter Province, Aus.	0.4	750–800, 0.6–0.7	92	15	80	85	(3)
Appalachians, N. Am.	0.4	1000, 1.0	57	18	39	43	(4)

[a] Crustal heat flow component at the time of metamorphism. References: (1) Heaman et al. (2011), Lévy et al. (2010), Jaupart et al. (2014), (2) Jones (1987, 1992), Andreoli et al. (2006), (3) McLaren et al. (2006), (4) Ague et al. (2012), Lévy et al. (2010), Lévy and Jaupart (2011).

Table 7
Average surface heat flux, $\bar{q_o}$, average crustal heat production, $\bar{A}$, crustal thickness, h_m, and differentiation index, DI, (Eq. (11)) for different provinces.

Province	Age (Gy)	$\overline{q_o} \pm \sigma$ (mW m^{-2})	$\overline{A} \pm \sigma$ (μW m^{-3})	h_m (km)	DI	Reference
Slave province, Can.	3.1	51	2.0	36	2.0	(1)
Superior craton core, Can.	>2.7	31.8 ± 5.2	0.78 ± 0.37	40	2.0	(2)
Superior accreted terranes, Can.	2.7	41.0 ± 8.7	0.8 ± 0.8	40	1.0	(2)
Wawa subprovince, Superior, Can.	2.7	45.1 ± 8.0	0.85 ± 0.79	40	1.0	(3)
Abitibi subprovince (all), Superior, Can.	2.7	39.9 ± 7.0	0.5 ± 0.4	38	0.7	(3)
Trans-Hudson Orogen, Can.	2.1–1.8	42 ± 11	0.7 ± 0.5	40	1.1	(2)
Flin-Flon Snow Lake Belt (THO), Can.	1.9–1.8	40 ± 5	0.32 ± 0.2	40	0.5	(3)
Wopmay Orogen, Can.	1.8	90 ± 15	4.8	32	2.0	(3), (4)
Central Shield, Aust.	1.8	72 ± 24	3.6 ± 1.9	35	3.2	(5), (6)
Eastern Gawler craton, Aust.	1.6	78 ± 19	5.0	40	2.4	(5), (6)
Grenville, Can.	1.3–1.1	41 ± 11	0.8	40	1.0	(3)
Namaqua, S. Africa	1.05	61 ± 11	2.3	43	2.0	(6), (7)
Appalachians, N. Am.	0.4	57 ± 13	2.6 ± 1.9	40	2.5	(3)

References: (1) Perry et al. (2006a), (2) Jaupart et al. (2014), (3) Perry et al. (2010), (4) Lewis et al. (2003), (5) Neumann et al. (2000), (6) Mareschal and Jaupart (2013), (7) Jones (1987, 1992).

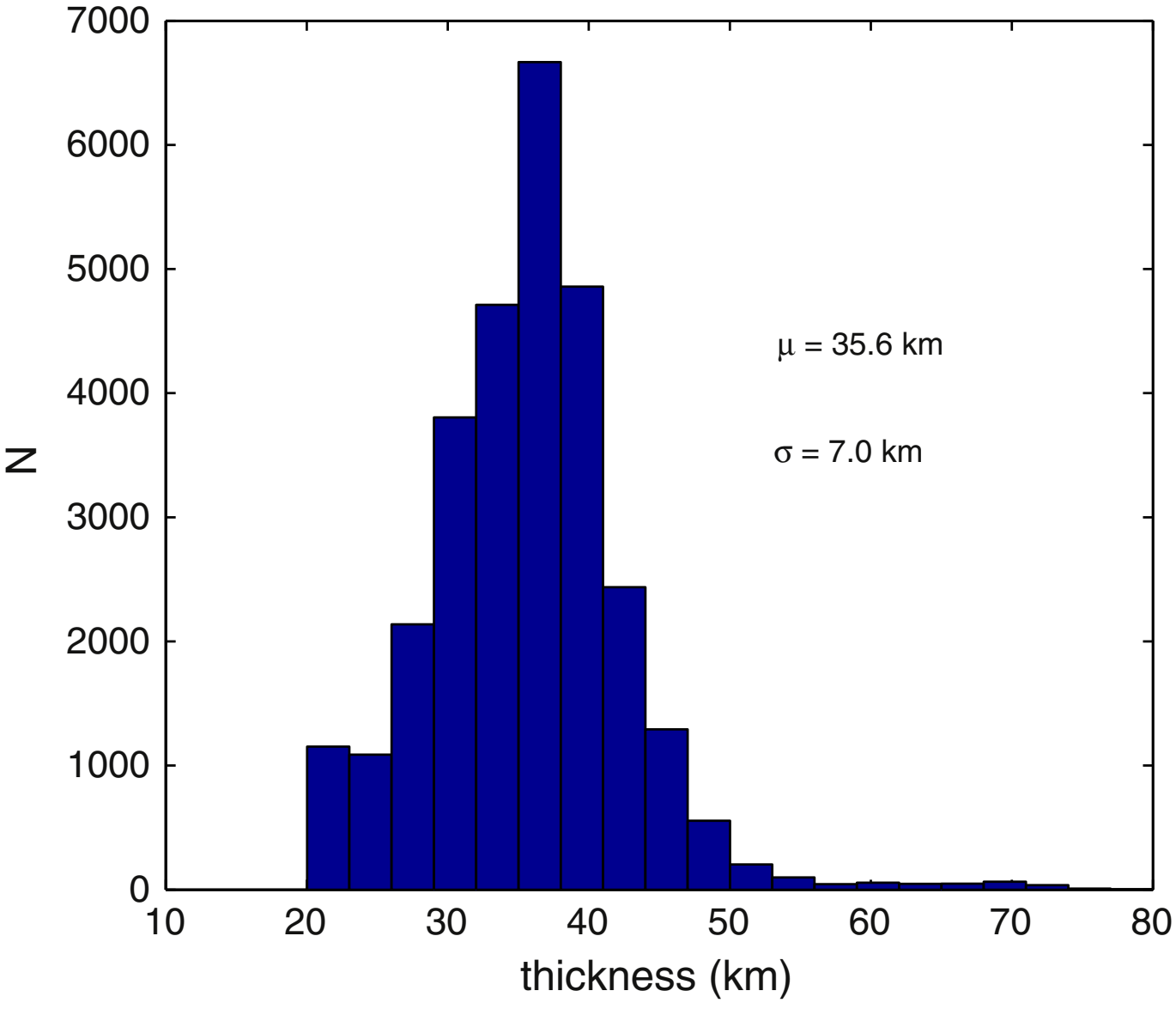

Fig. 12. Histogram of continental crust thicknesses sampled at 1° × 1° from Laske et al. (2013). Most of values >50 km or <30 km are in active regions.

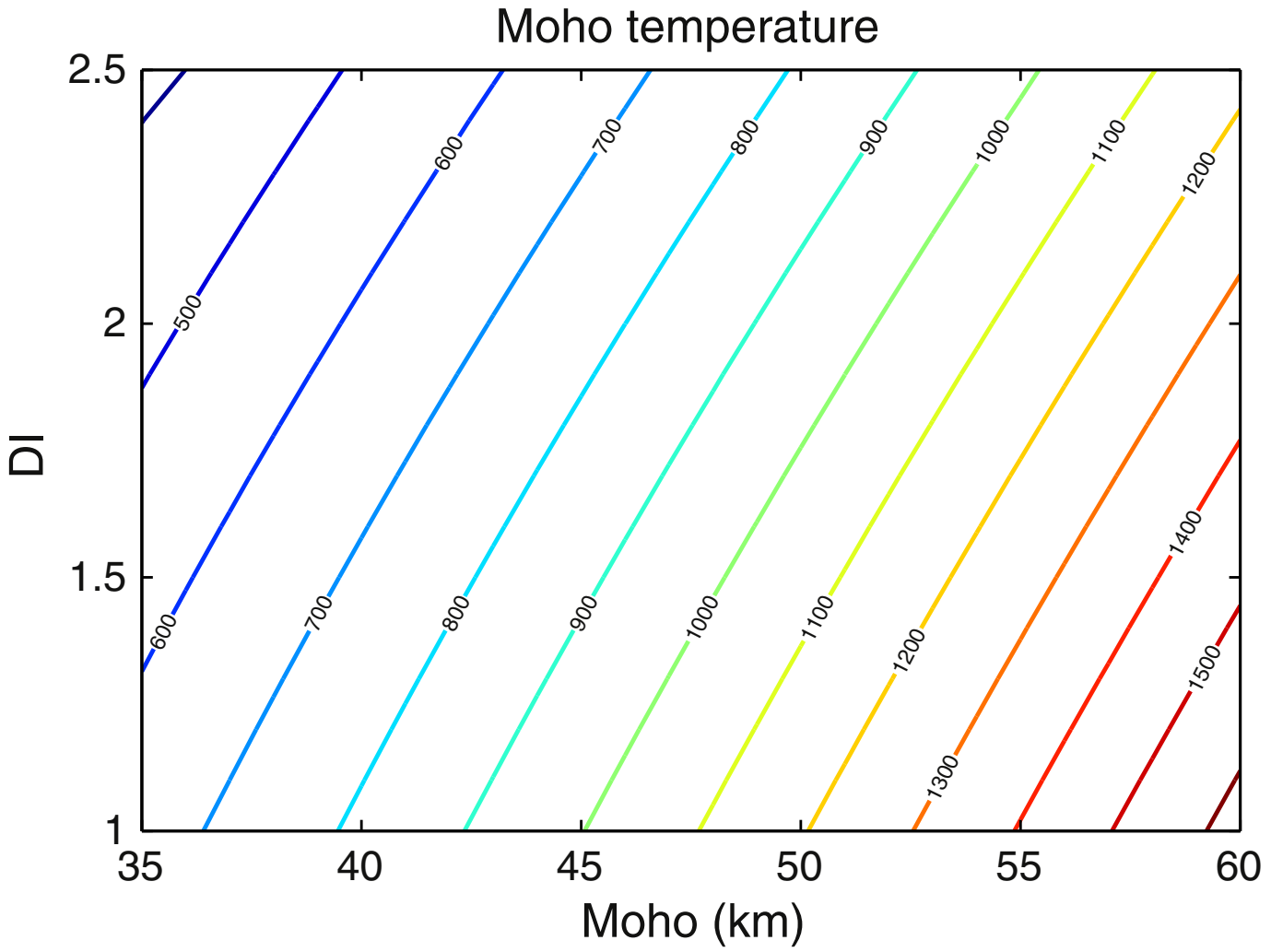

Fig. 13. Moho temperature variations in function of crustal thickness and differentiation index DI for a mean crustal heat production 1.5 μW m^{-3} representing Archean conditions.

results in a very implausible 1200 K increase in steady state Moho temperature, unless the heat producing elements are redistributed before steady state is reached. This redistribution can be achieved in two different ways: partial melting followed by upward segregation of the heat producing elements and/or lateral extrusion. If radioactive elements are brought near the surface as soon as partial melting occurs, temperatures remain close to solidus values (McKenzie and Priestley, 2016). In numerical models of the Himalayas that account for crustal heat production, lower parts of the thickened crust are mechanically weak because their temperatures are elevated, leading to lateral extrusion and exhumation (Beaumont et al., 2004). Regardless of the mechanism, the point is that self-heating of the crust plays a key role in the evolution of compressional orogens.

7.3. Strength of crust and lithosphere

For long-term survival at Earth's surface, a continent must be able to withstand tectonic perturbations and far-field deviatoric stresses without major deformation. Elevation differences at an ocean-continent boundary are associated with a force of ≈5 TN m^{-1} (McKenzie, 1977). Forces that arise from mantle convective processes manifest themselves as slab pull and ridge push, due to the negative buoyancy of subducting plates and the elevation of ocean ridges, respectively. Both are in a 2–5 TN m^{-1} range (Bott, 1989; Copley et al., 2010; Forsyth and Uyeda, 1975; Parsons and Richter, 1980). Stable continental lithosphere must be sufficiently strong to resist such forces. Following the standard approach summarized in Appendix D, we have calculated how the strength of the lithosphere varies with crustal thickness and differentiation for two different values of the average crustal heat production (1.1 and 1.5 μW m^{-3}). For the value of 1.5 μW m^{-3}, which represents the mean heat production of newborn Archean crust at 2.7 Ga (Jaupart et al., 2014), we find that undifferentiated crust of average thickness is too weak (Fig. 14a). The upward segregation of heat sources in an upper crustal layer, however, increases the lithospheric strength by a large factor and allows stabilization. Crust with an average heat production of 1.1 μW m^{-3}, which is that of the Appalachian mountains today, is considerably stronger than with 1.5 μW m^{-3} (Fig. 14b).

The same line of reasoning can be applied to the mechanical stability of belts with anomalously deep crust. Crustal thickening has two consequences which both tend to destabilize the lithosphere. It enhances the gravitational potential energy of the crust and thus generates tensile stresses. At the same time, it acts to raise temperatures in both the crust and the underlying mantle root, which reduces the integrated strength of the lithosphere and diminishes its capacity to withstand the tensile stress regime. In a first approximation, one may estimate the change of gravitational potential energy by assuming that the relationship between elevation and crustal thickness follows Airy's isostasy.

Considering only an average crustal density ρ_c and an average mantle density ρ_m, we have:

$$\delta h = \frac{\rho_m - \rho_c}{\rho_c}\delta h_m$$
$$\delta U = g(\rho_m - \rho_c)\delta h_m \times \left(h_m + \frac{1}{2}\delta h_m\right) \quad (14)$$

where δh is the elevation change due to a δh_m change in crustal thickness; h_m is an arbitrary reference crustal thickness, g is the acceleration of gravity. For $h_m = 40$ km, $\rho_c = 2850$ kg m^{-3} and $\rho_m = 3250$ kg m^{-3}, we have $\delta U/\delta h_m \approx 0.16$ TN m^{-1}/km. This force is compared to the total strength of the lithosphere in Fig. 14. For an average heat production of 1.5 μW m^{-3}, undifferentiated crust cannot withstand more than 5 km of crustal thickening without collapsing (Fig. 14a). Differentiated crust with an enriched upper layer can be thickened by up to 15 km without going unstable. This vertical differentiation can be achieved at constant bulk heat production by melting in the lower crust and extraction of felsic melts leading to enriched granitic intrusions in the upper crust. Alternatively, it can result from tectonic deformation, erosion and sedimentation (Sandiford and McLaren, 2002). With an average heat production of 1.1 μW m^{-3}, the strength of the crust is considerably higher than with 1.5 μW m^{-3}, but it decreases rapidly with increasing thickness. The tensile stress due to potential energy exceeds the strength of differentiated crust that is thicker than 60 km (Fig. 14b).

These simple calculations neglect thermal expansion in both crust and lithospheric mantle. Accounting for these effects would lead to larger differences in elevation and potential energy and would reinforce our conclusions. On a geological time-scale, the strength of the lithosphere increases as radioactive elements run down, so that a continent can sustain larger and larger elevation differences (Rey and Coltice, 2008).

7.4. Lower crustal flow

Horizontal variations of crustal thickness and elevation that are generated by continental collision or extension get relaxed rapidly on geological timescales, which has been explained by lower crustal flow (Bird, 1991; Buck, 1991). For this to occur, the viscosity of the lower crust must be sufficiently low, which requires temperatures of 700 °C or more (Hopper and Buck, 1993; McKenzie et al., 2000). This may be attributed to igneous intrusions or radioactive heating. We show below that temperatures can be high enough in the lower crust of many geological provinces due to local heat production. It is not our purpose to evaluate the effects of igneous intrusions but we remark briefly that they are short lived, which limits their relevance. According to McKenzie et al. (2000), for example, for lower crustal flow to smooth out crustal thickness variations in the eastern Great Basin, western USA, it must occur in a ≈ 10 km thick channel. If weakening is due to magma addition, temperature and viscosity return to their normal values in about 0.5 My (McKenzie et al., 2000). Viscosity would be at the required value only for a small part of that very brief time interval. There are several ways in which this model can be improved, involving for example sustained magmatic activity and concomitant lower crustal flow, but the point is that radioactive heating can do the trick and can be effective over long time intervals.

8. The role of crustal heat production in high-T metamorphism and crustal anatexis

The cause of high-T metamorphism, which is characterized by temperatures exceeding 800 °C at pressures in a 0.7–1.0 MPa range, has not been ascertained yet despite decades of research (Heaman et al., 2011). Many authors have called on the emplacement of large quantities of mafic magma in the crust, but this does not seem consistent with the time-lag of several tens of million years that separates metamorphic events from voluminous magmatism (Heaman et al., 2011; Krogh, 1993). Others have argued in favour of anomalously high rates of crustal heat production (Andreoli et al., 2006; Chamberlain and Sonder, 1990; Jaupart and Mareschal, 2015b; Kramers et al., 2001; McLaren et al., 2006; Kumar et al., 2007). We address this question in two different ways. In this section, we evaluate the amount of crustal heat production in several high-T provinces and show that they are elevated compared to global geochemical averages. We also discuss how to use present-day data in thermal models for past orogenic events. In the next section, we show that the thermal evolution of crust with high heat production is characterized by a late heating event that lags the cessation of orogenic activity by a few tens of million years.

8.1. Some general characteristics

Crustal heat production varies from province to province, implying that its relevance to high-T metamorphism cannot be assessed with generic models. Table 5 lists data for four geological provinces which span a large part of Earth's history, showing that high crustal temperatures are not specific to any particular geological era. After corrections for radioactive decay since the times of the orogenic events, values for the crustal heat flow component q_c are in the $43-85$ mW m^{-2} range, clearly higher that those of the "average" crusts of Table 1, which are in a $28-36$ mW m^{-2} range.

In recent models of the thermal evolution of continental crust during a cycle of tectonic thickening and erosion, Clark et al. (2011) have imposed zero heat production in the lower crust. With such an extreme distribution, they have effectively minimized the impact of crustal heat sources. A highly stratified crust with enriched granites at the top is a consequence of orogenesis and should not be taken as a realistic initial condition unless there is strong evidence to the contrary. Delving into the details of the time-dependent calculations by Clark et al. (2011) would be outside the scope of this paper and we only evaluate the consequences of their starting heat production model. Redistributing over the whole crustal thickness h_m heat sources that are concentrated in an upper layer of thickness h with heat production A_s leads to a uniform crustal heat production $A_c = A_s h/h_m$. For these two cases, crustal contributions to the Moho temperature are $A_s h^2/(2\lambda)$ and $A_c h_m^2/(2\lambda)$, respectively. The latter is larger than the former by a factor equal to h_m/h, or typically about 4. Enhancement factors would be smaller for distributions that are intermediate between these two (*i.e.* involving for example a mid-crustal layer) or higher for an enriched lower crustal layer.

8.2. The Appalachians province and the Acadian orogeny

Ague et al. (2012) have recently found evidence for ultra-high (≈ 1000 °C) metamorphism during the Devonian Acadian orogeny. Referring to calculations by Chamberlain and Sonder (1990), they have argued that overthickened crust is unable to produce the required thermal conditions. We show why these calculations underestimate the thermal conditions of the Acadian orogeny. Heat production data for the main rock types of the province are given in Table 8. We have verified that the present-day exposures are representative of large crustal volumes by turning to shales from the adjacent Atlantic continental margin, which were derived from Appalachian upper crustal material.

Fig. 14. Total strength of lithosphere *vs* crustal thickness. The strength is calculated for $DI = 1$ (undifferentiated) and $DI = 2.5$ (differentiated crust). The potential energy difference (relative to 40 km thick crust) is given for comparison. (a)The average crustal heat production is 1.5 μW m^{-3} (*i.e.*, the average heat production in cratons at the end of Archean). (b)The average crustal heat production is 1.1 μW m^{-3} (*i.e.*, the average heat production of the Appalachians at the time of the Acadian orogeny).

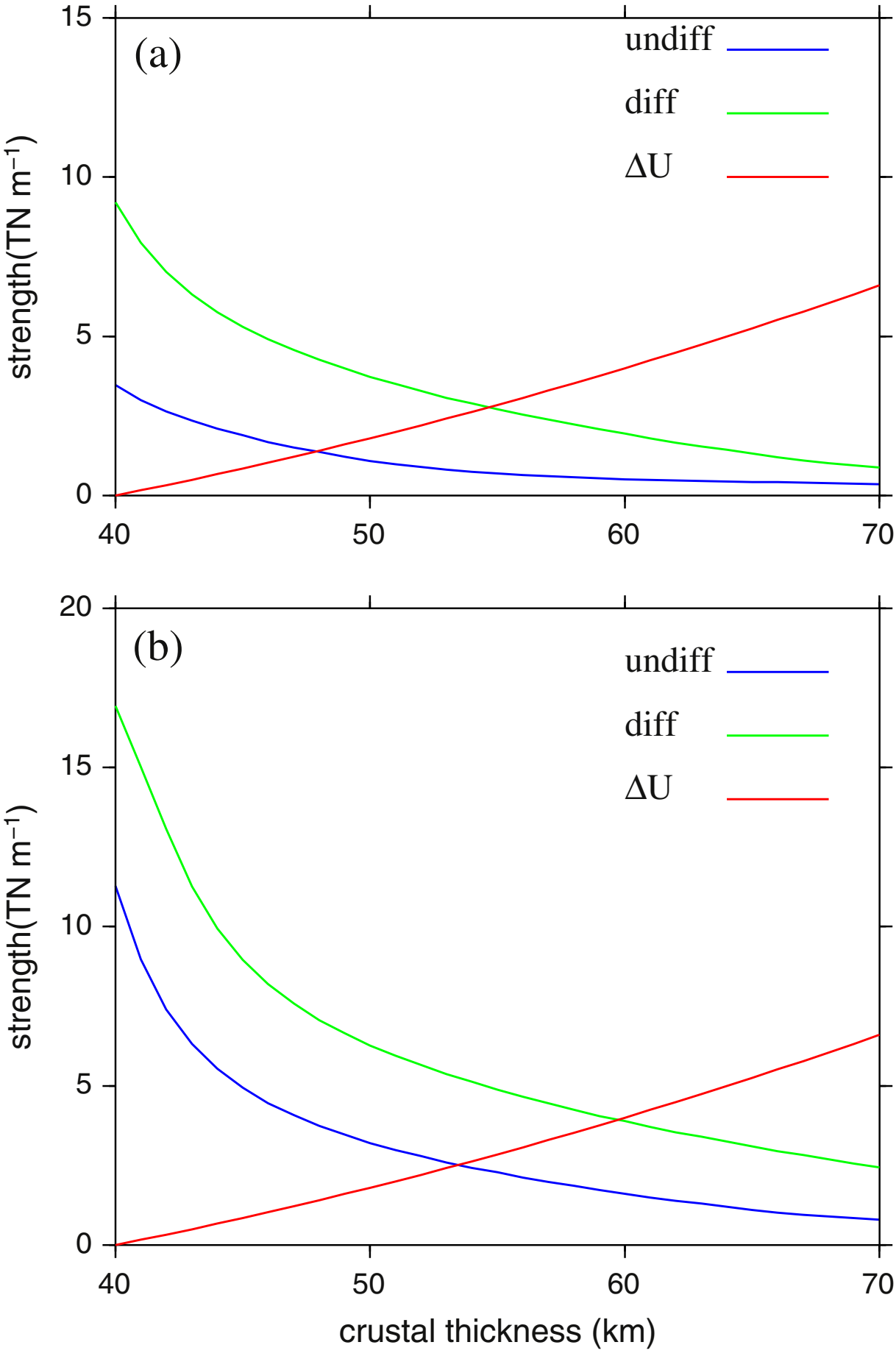
(a)
undiff
diff
ΔU
strength(TN m⁻¹)
15
10
5
0
40
50
60
70
(b)
undiff
diff
ΔU
strength(TN m⁻¹)
20
15
10
5
0
40
50
60
70
crustal thickness (km)

Table 8
Heat production data for the Appalachians province, U.S.A.

	A (μW m^{-3})	Reference
Large-scale surface average	2.6 ± 0.3	(1)
Shales[a]	2.15–2.37	(2)
Syntectonic plutons (410–390 Ma)[b]	1.8–2.2	(3), (4), (5)
Post-tectonic plutons (360 Ma)[c]	4.0	(6)
Anorogenic granites (*ca.* 180 Ma)[d]	8.6	(6)

References: (1) Jaupart and Mareschal (2014), (2) Della Vedova and Von Herzen (1987), (3) Chamberlain and Sonder (1990), (4) Lyons (1964), (5) Jaupart et al. (1982), (6) Roy et al. (1968).
[a] Sediments from the U.S. Atlantic continental margin (COST B-2 and B-3 boreholes).
[b] New Hampshire plutonic suite (three major plutons: Kinsman, Spaulding and Bethlehem gneiss).
[c] Concord two mica granites (several plutons scattered throughout New England).
[d] White Mountain plutonic series.

These shales have almost the same heat production as the currently exposed rocks (Table 8).

In their model, Chamberlain and Sonder (1990) took q_c = 35 mW m^{-2}, less than our best value of 43 mW m^{-2} at the time of metamorphism (Table 5). They also considered that heat production decreases exponentially with depth according to $A(z) = A_s \exp(-z/D)$ where z is depth and D = 10 km, leading to very low values in the lower crust (less than 0.17 μW m^{-3} for z > 30 km). All these assumptions err in the direction of lower temperatures. When dealing with the Acadian orogeny, the very concept of a highly stratified crust with depleted lower crust is questionable. The Appalachians crust is certainly stratified today, as shown by heat flow data, but its stratification is partly due to crustal melting and magma transport to the upper crust, in other words it is a consequence of the orogenic event itself. The large syntectonic intrusives of the New Hampshire plutonic suite and the highly radioactive post-tectonic Concord granites that are scattered throughout New England testify to both enrichment of the upper crust and depletion of the lower crust (Table 8). The Appalachian crust was modified further by the formation of the very enriched anorogenic plutons of the White Mountain Magma Series. The large amounts of uranium and thorium of these plutons are difficult to attribute to their parent mantle melts, all the more as they came from a depleted mantle source (Foland and Allen, 1991). Isotopic studies show that the White Mountains magmas have incorporated large amounts of pre-existing crust (Foland and Allen, 1991), thereby scavenging heat sources from the basement. Returning materials from the exposed intrusives to their original positions acts to enhance heat production deep down in the crust.

For the sake of discussion, we have calculated steady-state geotherms for several distributions of heat production. The Appalachian crust of today is 40 km thick and the mantle heat flux is probably as high as 18 mW m^{-2} (Lévy et al., 2010). Today, heat production in its approximately 10 km thick upper crust is 2.6 μW m^{-3} and the crustal heat flow component is 39 mW m^{-2}. We apply a small correction for the age of the Acadian orogeny (a 10% increase). For mid and lower crusts that are both 15 km thick, we have first taken heat production rates to be 0.7 and 0.3 μW m^{-3}, respectively, which are consistent with the global crustal models (Table 1). Using temperature-dependent conductivity (Appendix A), the predicted Moho temperature is 548 °C. The crust of today is thinner than at the end of the orogeny and sediments of the US continental margin show that the crust that was eroded away in the last 200 million years has the same heat production as today's surface average (Table 8). We can estimate the amount of denudation from the crystallization conditions of the White Mountains intrusives, which indicate pressures in a 0.1–0.15 GPa range. Adding 5 km of upper crustal material leads to a paleo Moho temperature of 733 °C. Redistributing heat sources over the vertical, the temperature at the base of a homogeneous crust would be 939 °C. These estimates provide bounds for the Moho temperature in the Appalachians and it is clear that even modest amounts of thickening would lead to the ultra-high metamorphic temperature reported by Ague et al. (2012).

8.3. The Archean Lewisian complex, northern Scotland

The Scourie granulitic rocks of northern Scotland were amongst the first ones to be recognized as exposures of the lower crust and are worth discussing because of their notoriety. These rocks were heated to 875–975 °C at pressures of 0.85–1.15 GPa about 2.8–2.7 Gy ago (Johnson and White, 2011). They are strongly depleted in uranium and thorium, which has led many authors to conclude that crustal heat sources did not play an important role (Rollinson, 2012).

The Scourie granulites are part of the Archean Lewisian complex which also includes the Torridon ampholite facies gneisses. The Scourie granulites and the Torridon amphibolites share the same geological history and have barely been affected by later deformation events. They provide samples of middle and lower crustal levels (Rollinson, 2012). Parts of the Lewisian upper crust have been preserved in local sedimentary rocks, notably in the Stoer Group mudstones (Kinnaird et al., 2007; Young, 1999) and probably in the Loch Maree clastic metasediments although this is controversial (Floyd et al., 1989; Park et al., 2001).

Table 9 lists data for the main rock types of the Lewisian complex and associated metasediments. The Stoer mudstones and Loch Maree shales have almost identical uranium and thorium contents. Heat production decreases steadily as one goes through the supracrustals-amphibolites-granulites sequence. In order to discuss the Lewisian crust in the Archean, we have corrected the present-day U, Th and K concentrations for radioactive decay (Table 9). The Archean heat production values do qualify as high by the standards of the global geochemical models (Table 1). In particular, with higher heat production than all the global estimates for the lower crust, the Scourie granulites no longer appear as exceptionally depleted. These granulites are in fact restites from a partial melting event that is dated at about the time of high-T metamorphim (Rollinson, 2012). Their protolith lost most of its uranium and thorium to melts that rose to shallower crustal levels. It is therefore an enhanced lower crustal heat production that should be entered in a thermal model for the metamorphic event.

For the sake of example, we have built a tentative Lewisian crustal column using the Stoer composition for the upper crust, the Torridon amphibolites for the middle crust and the Scourie granulites for the lower crust. The differences in layer thickness between global crustal models are small (see Table 1). Using three layers of 13.7, 13 and 12.1 km thicknesses, respectively, a Moho heat flux q_m = 15 mW m^{-2} and thermal conductivity from Appendix A, we find a Moho temperature of 714 °C at steady-state. This calculation is only valid for Lewisian crust whose deep layers had already been depleted and provides a lower bound for the Moho prior to intracrustal fractionation. For homogeneous crust with the same crustal heat flow component, the steady-state Moho temperature would be 988 °C. These estimates correspond

Table 9
Heat production data for the Lewisian-Scourie area, NW Scotland.

Rock type	U (ppm)	Th (ppm)	K (%)	A (present) (μW m^{-3})	A (2.7 Gy) (μW m^{-3})	Ref.
Loch Maree supracrustals[a]	3.19	11.1	2.1	1.83	3.46	(1)
Stoer mudstones[b]	3.2	8.2	2.3	1.64	3.30	(2)
Torridonian amphibolite gneisses	0.67	6.1	2.23	0.81	1.73	(3)
Scourie granulites	0.07	0.17	0.80	0.11	0.38	(3)

References: (1) Floyd et al. (1989), (2) Young (1999), (3) Rollinson (2012).
[a] Clastic metasediments derived partly from Archean basement of doubtful provenance (Park et al., 2001).
[b] Clastic sediments derived from local Lewisian basement (Kinnaird et al., 2007; Young, 1999).

to two extreme vertical distributions of heat production and define the range of Moho temperatures. These steady-state calculations may not capture accurately the thermal conditions of the Lewisian orogenic event, which saw the thickening of the crust and the burial of the Scourie protolith (Rollinson, 2012). They do indicate, however, that heat production in the Lewisian crust was probably large enough to account for high-T metamorphism.

9. Thermal transients

There are two types of thermal transients that are intrinsic to radiogenic heat production. One derives from the very process of radioactive decay, such heat production decreases with time as the unstable isotopes of uranium, thorium and potassium get progressively exhausted. The consequences for the thermal evolution of thick roots and for the interpretation of heat flow data have been studied in a series of papers (Jaupart and Mareschal, 1999, 2015a; Michaut et al., 2007, 2009). The other type of thermal transient has been described recently and arises in the aftermath of an orogenic event (Jaupart and Mareschal, 2015b).

9.1. Post-orogenic metamorphism and anatexis

Many ancient metamorphic events were followed quasi-isobaric cooling over long time intervals of 300 My or more, indicating negligible rates of denudation (Heaman et al., 2011; Mezger et al., 1990). We may therefore ignore erosion, which simplifies matters considerably. Post-orogenic thermal evolution is best understood by breaking down the temperature field in two components, which is possible for a constant thermal conductivity (Jaupart and Mareschal, 2015b):

$$T(z,t) = T_i(z,t) + T_r(z,t) \tag{15}$$

Component T_i describes the diffusive relaxation of the initial thermal structure $T_o(z)$, such that the initial condition is $T_i(z,0) = T_o(z)$. Component T_r accounts for crustal heat production and starts at zero by construction. The breakdown of temperature in these two components is not arbitrary, but the time of the breakdown is. One can begin the calculation at any time and the initial thermal structure $T_o(z)$ is a snapshot in an evolution that started earlier and that involved crustal heat production.

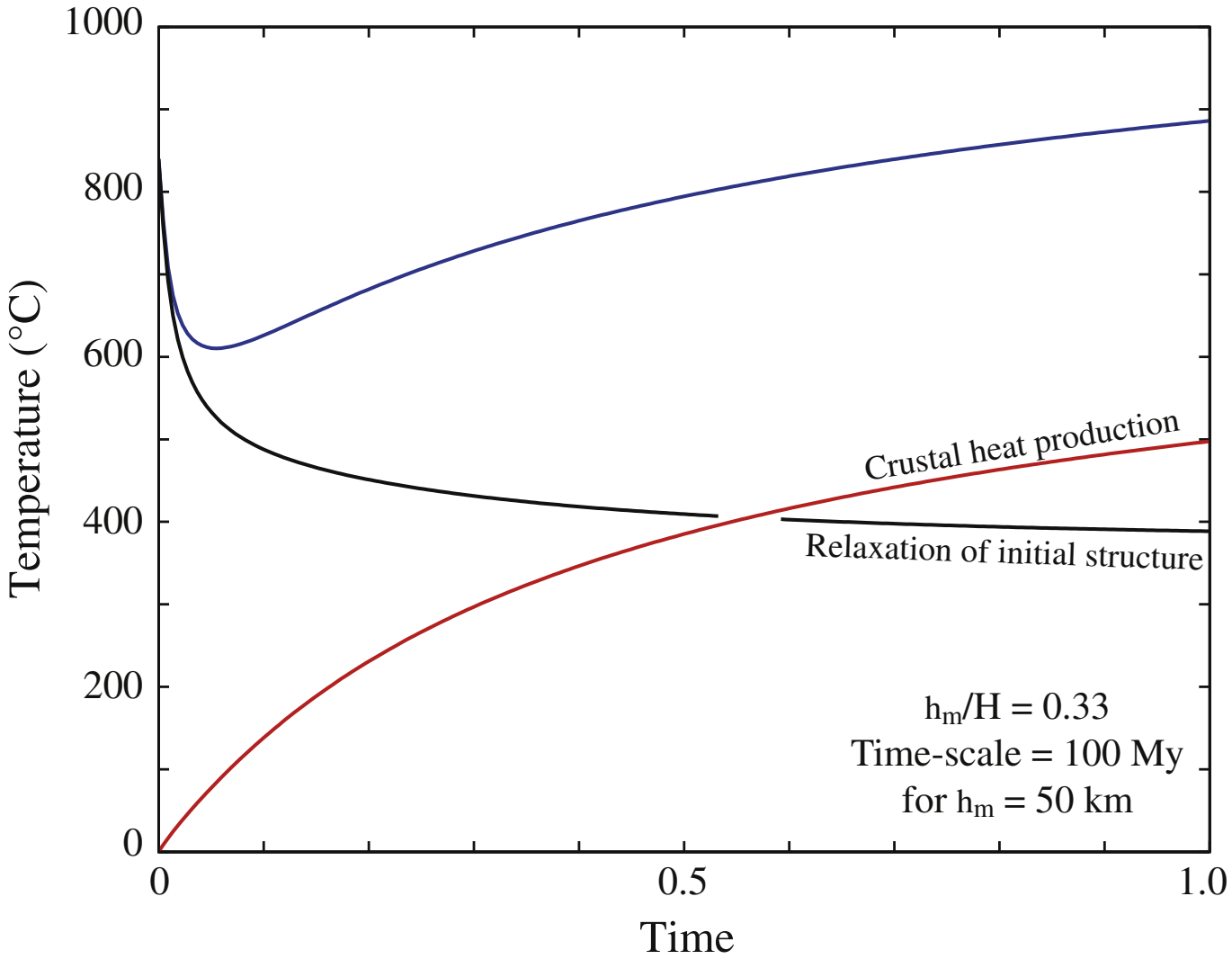

Fig. 15. Post-accretion thermal evolution of crust with an initial temperature anomaly confined to a lower crustal layer (blue line). Results are given for the lower crust ($z = 0.8 \times h_m$). The two temperature components T_i and T_r (Eq. (15)) are also shown. Crustal thickness $h_m = 50$ km, lithospheric thickness $H = 150$ km. The initial thermal structure is characterized by a deep crustal anomaly with a temperature of 850 °C between depths of 35 km and 50 km (base of the crust). Crustal heat production is 1.5 μW m^{-3}, as appropriate for juvenile Archean crust in the Superior Province of the Canadian Shield (Jaupart et al., 2014). The time-lag between the end of accretion and high-temperature metamorphism (T ≈ 850 °C) is ≈60 My.

The key aspect is that the two components evolve over two different time-scales, noted τ_i and τ_r respectively. τ_i depends on the vertical extent of the initial thermal anomaly and lumps together two transients: a fast one for an initial crustal anomaly such as a lower crustal "hot zone" and a slower one for perturbed lithosphere to return to equilibrium. τ_r is also set by the lithospheric response because the crustal sources must provide heat to both the crust and its underlying mantle root. Although both temperature components involve heat transport through the whole lithosphere, one has $\tau_r > \tau_i$ for the following reason. The thermal evolution depends on heat loss through the surface, which acts in opposite senses for the two components. It accelerates cooling and the thermal relaxation of the initial anomaly, but it slows down heating by crustal heat production. Starting from an initial "hot geotherm", as appropriate for the end of the orogenic event proper (*i.e.* the end of tectonic deformation and magmatic activity from external sources), one observes an initial cooling phase that gets interrupted by radiogenic heating. With sufficiently large values of heat production, one may return, or even exceed, the starting values of temperature in the crust, which accounts for post-orogenic metamorphism and plutonic activity. As shown by Jaupart and Mareschal (2015b), the time-lag between the end of the orogeny and post-orogenic peak metamorphism is predicted to be several tens of million years, in agreement with the observations (Heaman et al., 2011).

One set of results from Jaupart and Mareschal (2015b) is shown in Fig. 15 for 150 km-thick lithosphere. Heating by crustal heat sources overwhelms the initial cooling after a time of about 10 My and temperatures in the lower crust rise to values larger than 850 °C after about 60 My. This time lag would be shorter for a smaller initial thermal perturbation and higher heat production, and it would be longer for a smaller heat production. It is worth illustrating how the radioactive temperature component T_r evolves during the post-orogenic thermal ramp-up (Fig. 16). In a first phase, temperatures rise steadily everywhere with a peak just above the Moho because the heat sources are located in the crust and shed heat to the underlying lithospheric mantle. This phase segues into a second one characterized by the slow evolution of the lithospheric root towards thermal equilibrium with the crustal heat sources. Once this has been achieved, one enters a phase of secular cooling due to the rundown of radioactivity, which is described next.

9.2. Secular changes of lithospheric temperatures

Following the thermal relaxation of the initial lithosphere formation event, two types of long-term transients may occur, due to changes of heat supply at the base of the lithosphere and to the rundown of radiogenic heat production. We restrict our attention to crustal heat sources and ignore lithospheric ones, whose effects have been described in several papers (Jaupart and Mareschal, 1999; Michaut and Jaupart, 2007; Michaut et al., 2007). The thermal relaxation time of thick continental lithosphere, $\tau_{diff} = H^2/\kappa$, where H is thickness and κ thermal diffusivity,

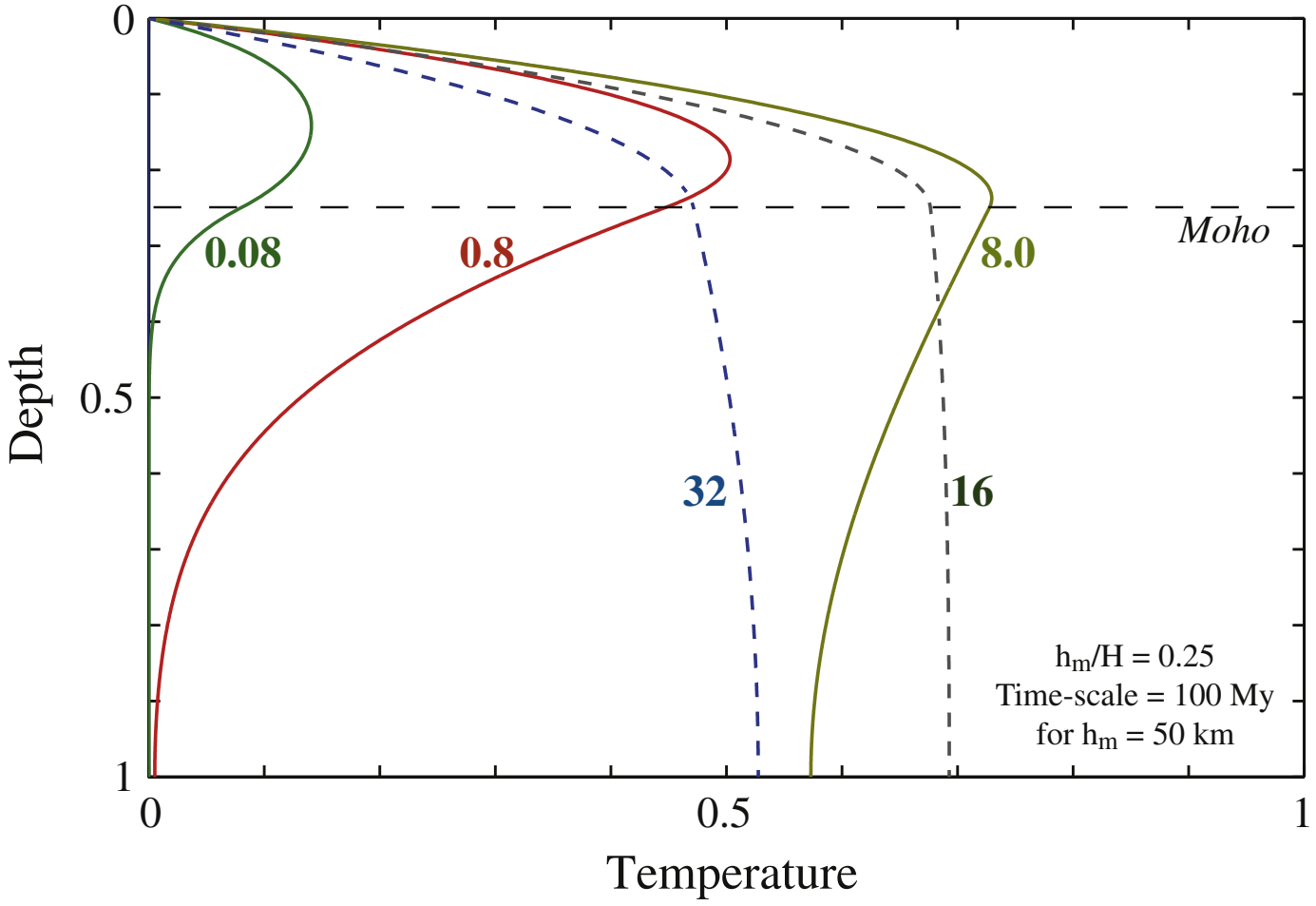

Fig. 16. Vertical temperature profiles illustrating the heating of the crust and lithosphere by crustal heat sources. Heat production decays according to the $A(t) = A_o \exp(-t/\tau_r)$, where $\tau_r = 3.4$ Gy. Temperature has been scaled to $A_o h_m^2/(2\lambda)$, which is the Moho temperature for a uniform and steady crustal heat production equal to A_o. The labels by the curves refer to times scaled to the crustal diffusive time-scale, ≈100 My for 50 km thick crust. The thermal evolution can be split in two different phases. In an initial phase, temperatures increase everywhere, with the lithospheric mantle lagging behind the radioactive crust. As a consequence, the maximum temperature is reached in the lower crust and not at the Moho. In a second phase, with profiles shown as dashed lines, the whole lithospheric mantle has been heated up but the decay of heat production induces generalized secular cooling.

is very large. For $H = 200$ km and $\kappa = 8 \times 10^{-7}$ m^2 s^{-1}, $\tau_{diff} = 1.6$ Gy. Such a very long time is responsible for peculiar thermal transients.

We first focus on heat production and its impact on the lithospheric geotherm, which we describe with the T_r temperature component. It takes a very long time for thick lithosphere to reach a regime of quasi-equilibrium with the crustal heat sources. For bulk Earth Th/U and K/U ratios, heat production follows closely an exponential decay with time constant $\tau_{radio} \approx 3.4$ Gy. This is not much larger than the diffusive relaxation time, implying that heat production decreases whilst lithospheric temperatures are catching up with the deep crust. Once secular quasi-equilibrium conditions have been attained, temperatures decrease everywhere (*i.e.* in both crust and lithospheric mantle) due to radioactive decay. Lithospheric temperatures therefore peak at a late time which increases with increasing lithosphere thickness (Fig. 17).

The slow decrease of lithospheric temperatures proceeds at a rate which is set by the decay of the radiogenic isotopes. For a typical value of crustal heat production of 0.7 μW m^{-3} today, corresponding to 1.5 μW m^{-3} at the end of the Archean, this rate is about 100 K/Gy. This is within the range of values for the secular cooling of the Earth's mantle (Jaupart et al., 2015), which raises interesting possibilities. The lithospheric root may cool down more rapidly than the underlying mantle, which may induce its thickening. It may also cool down less rapidly than the underlying mantle. In this case, the lithospheric geotherm would turn at some depth, such that the deep lithosphere would in fact be supplying heat to the asthenosphere. This lower lithospheric region would be stably stratified thermally, but it would lie beneath a hotter and mechanically weak horizon, which would favour shearing and delamination. These possibilities have been studied in more detail by Michaut et al. (2009).

The geological implications of these transient behaviours are multifold. Changes in the amount and/or vertical distribution of crustal heat sources that are induced by an orogenic event are rapidly translated into the thermal structure of the crust but can only affect the deep lithosphere after a long time lag. The crust and its thick lithospheric root may therefore remain thermally and mechanically decoupled for longer than the time between two orogenic events. In addition, the lower parts of lithospheric roots may be much more active than commonly thought.

10. Conclusion

The contribution of crustal heat sources to the surface heat flux remains insufficiently constrained. The range of global averages of heat production rates is wide (0.2 μW m^{-3}) and translates into an uncertainty of ± 4 mW m^{-2} for the crustal component and Moho heat flux. This is

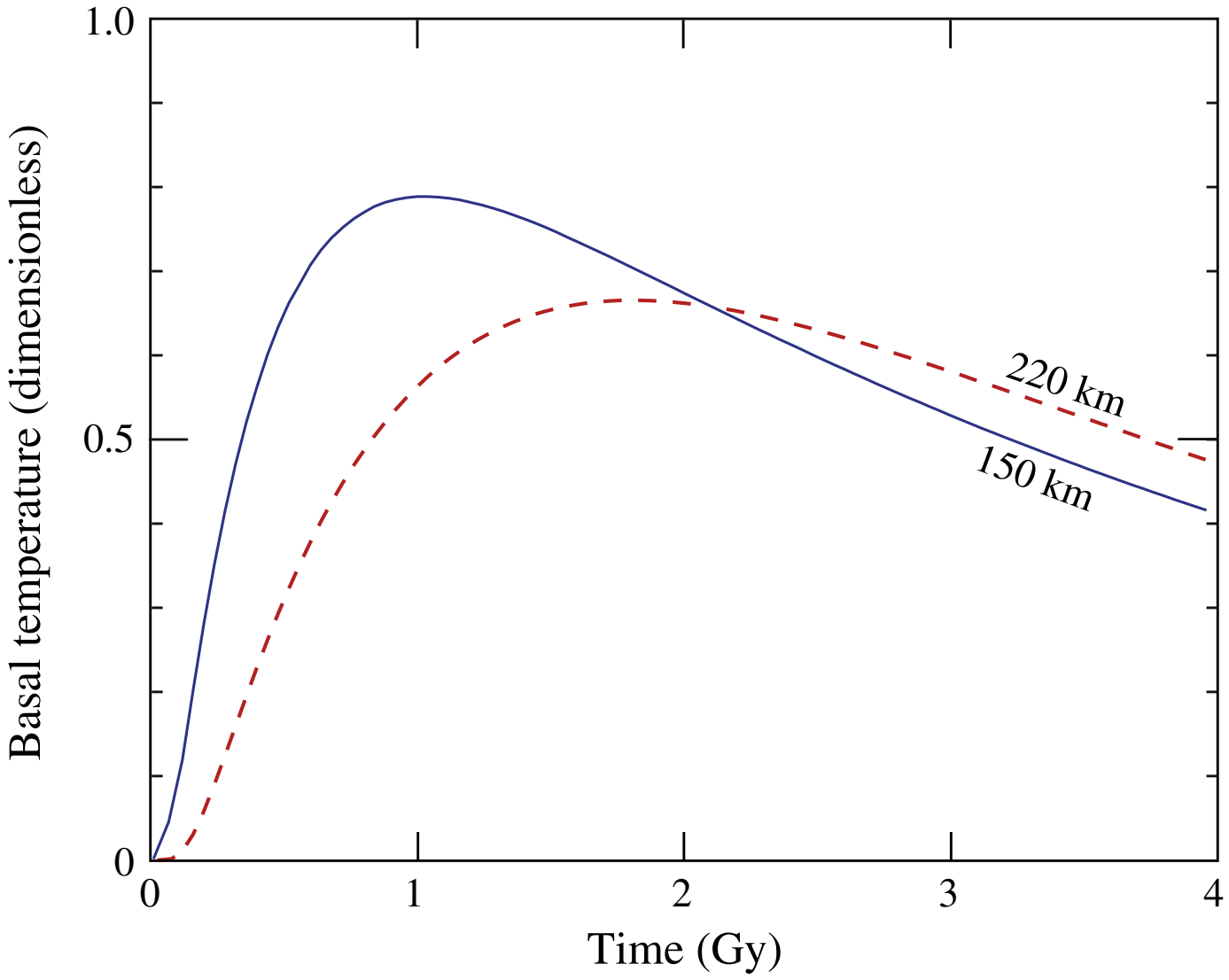

Fig. 17. Variation of temperature at the base of the lithosphere due to crustal heat production for two different values of the lithosphere thickness, 150 and 220 km. The true basal temperature also includes a transient component that is due to the thermal relaxation of the lithosphere-forming event (not shown here). Heat production decays according to the $A(t) = A_o \exp(-t/\tau_{radio})$, where $\tau_{radio} = 3.4$ Gy. Temperature has been scaled to $A_o h_m^2/(2\lambda)$, which is the Moho temperature for a uniform and steady crustal heat production equal to A_o.

comparable to the uncertainty associated with heat flow and heat production studies. It should be emphasized, however, that the Moho heat flux can only vary on scales of 500 km or more, so that heat flow studies allow the resolution of local variations in the crustal heat flow component within a province. Long wavelength variations of heat production in the lower crust are difficult to detect but they would have a strong effect on Moho temperatures if they exist. For a given surface heat flux, as far as lower crustal temperatures are concerned, overestimating present Moho heat flux is balanced by underestimating lower crustal heat production. But this compensating effect might not hold for reconstructing past conditions, when heat production was higher than today. Although not the focus of this review, the mantle heat flux value determines lithospheric temperatures and thickness with implications for interpreting seismic velocity profiles and xenoliths thermo-barometry data. Reciprocally, xenoliths and seismic studies are useful to validate the thermal models of the lithosphere. Attractive as the concept of thermal isostasy might appear, it is difficult to apply in the tectonically active regions that provide a large part of the elevation signal owing to their transient thermal structures.

We have emphasized the effect of crustal differentiation and lower crustal heat production on the thermal regime, strength and stability of the lithosphere. In addition, one must be aware that the crustal thickness should not be treated as a given but should rather be considered as resulting from a complex sequence of melting, intracrustal fractionation, and deformation events.

High rates of crustal heat production have been found in several regions that experienced high temperature metamorphism in the past. For the examples examined in this study, crustal heat production is largely sufficient to explain such metamorphic events without calling for an external thermal perturbation. Likewise, the 20–100 My delay between tectonic events, such as crustal accretion and compressional orogenies on the one hand and peak metamorphism on the other hand, is consistent with crustal self-heating by radiogenic elements.

Acknowledgement

The authors are grateful to Javier Ruiz and an anonymous reviewer for their very constructive and useful comments. This research was supported by INSU,CNRS (France) and by NSERC (Canada) (1443/2010).

Appendix A. Thermal conductivity

According to the metamorphic and plutonic records, the temperatures of crustal rocks may vary within a very large range of ≈0–1000 °C. Over this temperature range, phonons are the main energy carriers and the contribution of photons is expected to be small. The variation of lattice conductivity with temperature has been determined for a number of minerals and rocks with different techniques (Durham et al., 1987; Merriman et al., 2013; Miao et al., 2014). The inherent heterogeneity of natural rocks is responsible for large variations of conductivity, even for a single rock type.

Measurements on a suite of rock samples from the Canadian Shield over a (≈0–400 °C) temperature range by Durham et al. (1987) can be accounted for by relationship of the following form:

$$\lambda = 2.264 - \frac{618.2}{T} + \lambda_0 \times \left(\frac{355.576}{T} - 0.30247\right) \quad (A.1)$$

where T is the absolute temperature in Kelvins and λ_0 is the thermal conductivity at 0 °C. According to this equation, the lattice conductivity decreases with increasing temperature and tends to a constant value at high temperatures, which has been confirmed by more recent measurements (Merriman et al., 2013; Miao et al., 2014).

According to Merriman et al. (2013), the lattice conductivities of several crustal rock types, including granulite, greenstone and tonalite-trondhjemite-granodiorite (TTG), are confined to a small 1.9–2.2 W $m^{-1}K^{-1}$ range at temperatures larger than 700 °C. In the same high-T limit, Miao et al. (2014) report a much lower range of 1.26–1.55 W $m^{-1}K^{-1}$ for granite, granodiorite, gabbro and garnet amphibolite samples. This discrepancy may be due to anomalous samples. For example, Merriman et al. (2013) report a value of 4.5 W $m^{-1}K^{-1}$ for a TTG sample at room temperature, which is far above the range of previously published values for similar rocks. Similarly, Miao et al. (2014) quote a room temperature value of 1.92 W $m^{-1}K^{-1}$ for a granodiorite sample, which is this time significantly lower than all the measurements that are known to us on similar rocks. It may also be compared to the Merriman et al. (2013) value for a TTG sample, because both rocks belong to the same group. We have therefore excluded the data for these two particular samples. For the two suites of crustal rocks that were studied by these two groups, the range of conductivity values, which may be as high as 70% at room temperature, is only about 20% for $300<T<1000$ °C. As a result, thermal calculations are weakly sensitive to the choice of a representative crustal rock type.

Miao et al. (2014) have derived best-fit relationships to their conductivity data of the form $\lambda = (\alpha + \beta T)^{-1}$, where α and β depend on rock type and T is temperature in Kelvins. For $T>700$ °C, the measurements do not resolve any significant change of conductivity and this relationship should not be used. Merriman et al. (2013) list empirical equations for both diffusivity and heat capacity which lead to more complicated expressions for conductivity.

The continental crust is a complex assemblage of different rock types in both the horizontal and vertical directions and this must be accounted for in the choice of a representative thermal conductivity. We find that Eq. (A.1) represents a good compromise. It is very close to all the Durham et al. (1987) data by construction. For $\lambda_0 =$ 2.8 W $m^{-1}K^{-1}$, it predicts conductivity values that are within 20% of those of Miao et al. (2014) and Merriman et al. (2013) in the 0–900 °C range (Fig. 18). We have used this equation to calculate numerically Moho temperature T_m as a function of surface heat flux assuming homogeneous crustal heat production and a Moho heat flux of 15 mW m^{-2}. We then determined the effective thermal conductivity

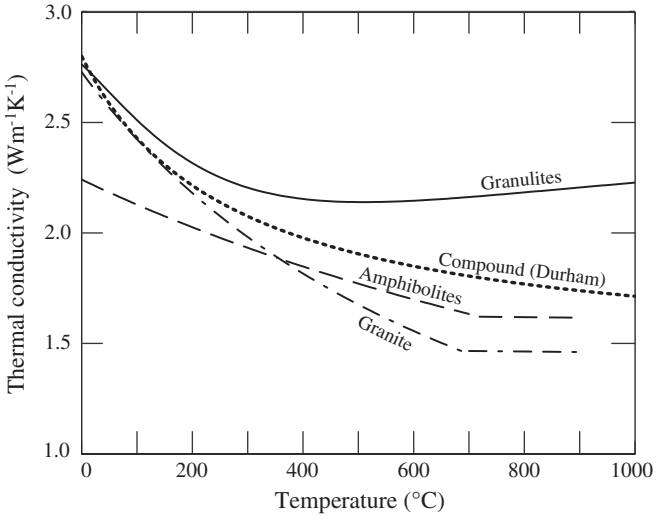

Fig. 18. Variation of the lattice component of thermal conductivity as a function of temperature for several representative crustal rocks. The dotted line corresponds to empirical relationship A.1 for a conductivity value of 2.8 W $m^{-1}K^{-1}$ at room temperature. This relationship was derived from a best-fit analysis of seven different rock samples from the Archean Superior province (Durham et al., 1987). The data for amphibolites and granite samples are from Miao et al. (2014). For these two samples, the measurements do not resolve any significant variations of thermal conductivity in the 700–900 °C range. The granulite data are from Merriman et al. (2013).

of the crust, λ_e, as the constant conductivity that yields the same Moho temperature as:

$$\lambda_e = \frac{(q_0 + q_m) \times z_m}{2 \times (T_m - T_0)} \quad (A.2)$$

We found that for a surface conductivity of 3 $Wm^{-1}K^{-1}$, T_m varies between 430 and 870 °C and λ_e varies between 2.3 and 2.1 W $m^{-1}K^{-1}$. Changing the surface conductivity by ± 0.2 W $m^{-1}K^{-1}$ results in <0.1 W $m^{-1}K^{-1}$ change in λ_e.

Appendix B. Moho heat flux

The first heat flow measurements were made on the continents, well before the advent of plate tectonics. It is therefore not surprising that early interpretations were focused mostly on crustal heat production. For example, Birch (1950) concluded from very imperfect heat flow, heat production, and gravity data that heat flow variations are due to changes in crustal structure and composition. He estimated that the heat flux at the base of the crust is ≈ 12 mW m^{-2} which, as we shall see, was not far off the mark. Estimates of the Moho heat flux in continental regions are based on heat flow and heat production data, systematic geochemical sampling, geothermobarometric studies on mantle xenoliths, as well as studies of crustal and lithospheric structure with seismic and electromagnetic methods.

An obvious constraint on Moho heat flux is that it must be less than the lowest value that is measured at the surface. Values as low as 18–22 mW m^{-2} have been measured in several Shield areas (Table 10). A value of 22 mW m^{-2} has been found in three widely separated regions in the Canadian Shield: in the *ca.* 2800 Ma LaGrande belt of the Superior Province, in the Lynn Lake belt of the *ca.* 1800 Ma Trans Hudson Orogen and at Voisey Bay in the *ca.* 1650 Ma Nain plutonic province. Because the heat production rate at these sites is not negligible, the Moho heat flux must be less than these values. In an extreme model, we consider that heat production in the whole crust beneath the measurement sites is equal to the lowest value observed on crustal rocks, which is 0.10 μW m^{-3} (Tables 1 and 6). For crust of average thickness (40 km), therefore, the Moho heat flux must be less than 14–18 mW m^{-2}. Similarly low values of Moho heat flux have been reported in other continents (Table 11).

The contribution of crustal heat sources can be estimated from crustal sections where deep crustal levels are exposed at the surface. For example, this is the situation of Kapuskasing structural zone in the Superior Province of the Canadian Shield where the crust is exposed to paleo-pressures up to 1 GPa (Percival and West, 1994). The surface heat flux measured in the region where the metamorphic grade is highest is 33 mW m^{-2} and the measured heat production of the granulites is 0.4 μW m^{-3} (Table 6). The crustal thickness was estimated to be 50 km from the seismic reflection and refraction surveys conducted by the LITHOPROBE program. Assuming that the granulites at the surface are representative of the present-day lower crust, we calculate a mantle heat flux of 13 mW m^{-2}. This result has been checked in different ways. The Kapuskasing structure lies at the western termination of the Abitibi subprovince where seismic reflection and refraction profiles as well as gravity data are available, and where many heat flow data have been collected. Using the physical properties of the main rock types of the province, Guillou et al. (1994) used a Monte-Carlo method to find crustal models that fit the heat flux, gravity, and crustal thickness variations between eastern, western, and southernmost parts of the Abitibi. They found that the range of Moho heat flux values is narrow (11–18 mW m^{-2}) and strongly peaked at 14 mW m^{-2}.

The total crustal heat production and the mantle heat flux have also been estimated in the Vredefort structure in the Kaapvaal craton, South-Africa (Nicolaysen et al., 1981) where a section of the entire crust has been exposed by the rebound following a meteorite impact *ca.* 2100 Ma. Nicolaysen et al. (1981) sampled a transect across the structure and estimated the total crustal heat production to be between 29 and 34 mW m^{-2} and the Moho heat flux to be 12–17 mW m^{-2}.

Mantle temperature-depth profiles can be calculated from geothermobarometry studies of xenoliths brought to the surface by kimberlite eruptions. Studies based on the same thermobarometers yield consistent temperature gradients in the mantle (Grütter, 2009). Unfortunately, many authors still try to obtain a qualitative fit of the P–T data to a "reference surface heat flow geotherm" such as proposed by Pollack and Chapman (1977), rather than directly estimate the mantle heat flux from the temperature gradient and thermal conductivity. The limitations of such a procedure is made evident when the entire P–T array cannot be fit by the same "reference geotherm" but is intersected by different geotherms at different depths (see for instance Sand et al., 2009). When the mantle heat flux has been calculated, its values in cratonic areas range between 10 and 20 mW m^{-2} (Table 11). The slightly higher values (15–22 mW m^{-2}) that have been obtained for South Africa (Michaut et al., 2007; Rudnick and Nyblade, 1999) are consistent with the range of 12–17 mW m^{-2} that was derived from surface heat flux and crustal heat production.

The crustal heat production models (and values of the Moho heat flux) have also been tested against P_n seismic velocity obtained from the LITHOPROBE seismic refraction profiles in the western Superior Province in Canada. Perry et al. (2006b) calculated Moho temperatures and P_n velocities for different mantle compositions. They found a best fit between 12 mW m^{-2} and 15 mW m^{-2} depending on the amount of mantle depletion. On a larger scale, Lévy et al. (2010) narrowed down to 12–18 mW m^{-2} the range of mantle heat flux values beneath central and eastern Canada using a combination of heat flux and shear wave

Table 10
Lowest surface heat flux measurements.

Location	Age (My)	Heat flux (mW m^{-2})	Reference
West African Shield		18–22	(1)
Lynn Lake (Trans Hudson, Canada)	1800	22	(2)
Voisey Bay (Nain, Canada)	1600	22	(3)
LaGrande (Superior, Canada)	2700	22	(4)
Ukrainian Shield		20	(5)
Dharwar craton (India)	2700	23	(6)
Baltic Shield		18	(7)
Urals	400	20	(8)
Siberian platform		12	(9)

(1) Chapman and Pollack (1974), (2) Rolandone et al. (2002), (3) Mareschal et al. (2000b), (4) Lévy et al. (2010), (5) Kutas (1977), (6) Roy and Rao (2000), (7) Kukkonen (1989), (8) Kukkonen et al. (1997), (9) Duchkov (1991).

Table 11
Moho heat flux (q_m) in different regions.

Location	Age (My)	q_m (mW m^{-2})	Reference
Kapuskasing (Superior, Canada)	1900	15	(1)
Abitibi subprovince (Superior, Canada)	2700	14	(2)
Grenville Province (Canada)	1100	14	(1)
Appalachians	400	18	(3)
Slave Province (Canada)	2700	11	(4)[a]
Dharwar craton (India)	2700	12–18	(5)
Baltic Shield	2700	12	(6), (7)[a]
Siberian platform		12	(8)
Altai-Sayan belt (Siberia)	450	10	(8)
Vredefort (South Africa)	2200	12–17	(9)
Kaapvaal (South Africa)		18–22	(10)[a]
Kaapvaal (South Africa)		14–18	(11)[a]
Sierra Nevada (USA)	200	<20	(12)
Sierra Nevada (USA)	200	10	(13)

References: (1) Pinet et al. (1991), (2) Guillou et al. (1994), (3) Lévy et al. (2010), (4) Russell et al. (2001), (5) Roy and Rao (2003), (6) Kukkonen and Jõeleht (1996), (7) Kukkonen and Peltonen (1999), (8) Duchkov (1991), (9) Nicolaysen et al. (1981), (10) Rudnick and Nyblade (1999), (11) Michaut et al. (2007), (12) Saltus and Lachenbruch (1991), (13) Brady et al. (2006).

[a] Estimated from surface heat flow and geothermobarometry on mantle xenoliths.

vertical travel time delays calculated from surface wave tomography models (Bedle and van der Lee, 2009).

Appendix C. Horizontal variations in heat sources

We assume that the horizontal distribution of heat production remains the same over some thickness h, and use calculations for elementary periodic distributions in the horizontal plane. These distributions are characterized by function $f(x,y)$ such that:

$$\nabla_H^2 f(x,y) = \frac{\partial^2 f}{\partial x^2} + \frac{\partial^2 f}{\partial y^2} = -k^2 f \tag{C.1}$$

where k is the equivalent of a wavenumber. Functions f that are solutions of Eq. (C.1) are such that their horizontal average is zero and can be understood as components of the 2-D Fourier transform in x and y of the heat production distribution $\delta A(x,y,z)$. They allow a wide range of periodic tesselations of the plane, including equally spaced parallel lines, squares and hexagons. For simplicity, we shall refer to a single scale or wavelength Δ such that:

$$k = \frac{2\pi}{\Delta} \tag{C.2}$$

For the heat equation with constant thermal conductivity, which is linear in T and A, we need only solve the problem for a layer that extends from the surface to depth h in a crust of total thickness h_m. Results for a layer located between depths z_T and z_B can be obtained by subtracting the solution for $h = z_T$ from that for $h = z_B$.

For an elementary heat production distribution $\delta A = A_o f(x,y)$, solutions can be obtained in the form of $T(x,y,z) = \theta(z) f(x,y)$, such that:

$$\frac{d^2\theta}{dz^2} - k^2\theta + \frac{A_o}{\lambda} = 0 \tag{C.3}$$

where A_o is set to zero below the layer of thickness h. For this problem, which deals with fluctuations of heat production around the horizontal mean, the following boundary conditions must be satisfied:

$$\begin{aligned} \theta(0) &= 0, \quad \text{zero surface temperature} \\ \frac{d\theta}{dz}(z = h_m) &= 0, \quad \text{zero heat flux at the Moho} \end{aligned} \tag{C.4}$$

Solutions are derived using standard mathematical methods. The surface heat flux is:

$$\delta q_o = A_o h \, \frac{\sinh(kh) + [1 - \cosh(kh)]\tanh(kh_m)}{kh} \tag{C.5}$$

For simplicity, it is useful to scale the heat flux with the value for a layer of constant heat production, $i.e. A_o h$. The Moho temperature is:

$$\delta T_m = \frac{A_o h^2}{\lambda} \, \frac{\cosh(kh) - 1}{k^2 h^2 \cosh(kh_m)} \tag{C.6}$$

As above, the Moho temperature will be scaled to the value for a layer of constant heat production, $(A_o h^2)/2\lambda$.

Appendix D. Rheology and strength of the lithosphere

Crustal rocks deform by power law creep (Ranalli, 1995)

$$\dot{\epsilon} = A\sigma^n \exp(-(E + PV^*)/RT) \tag{D.1}$$

where $\dot{\epsilon}$ is the strain rate, σ the deviatoric stress, A and n are constants characteristic of the material, E is the activation energy, V^* the activation volume, R the gas constant, P is pressure, and T temperature. In general, the strength is defined as the stress required to maintain a fixed rate of deformation $\dot{\epsilon}$, typically $10^{-15}\,s^{-1}$, which is a value commonly observed for tectonic deformations.

Table 12
Creep parameters for lithospheric materials used in calculating the strength of the lithosphere (Carter and Tsenn, 1987; Ranalli, 1995).

	A (MPa $^{-n}$s $^{-1}$)	n	E (kJ mol $^{-1}$)	ρ (kg m $^{-3}$)
Upper crust (dry granite)	1.0×10^{-7}	3.2	144	2700
Lower crust (mafic granulites)	1.4×10^{4}	4.2	445	2700
Mantle (dry dunite)	3.0×10^{4}	3.6	535	3300

$$\sigma = \frac{\dot{\epsilon}^{1/n}}{A^{1/n}} \exp((E + PV^*)/nRT) \tag{D.2}$$

We use parameters that correspond to dry rheologies for the crust and mantle (Table 12).

In the upper crust, deformation occurs by frictional sliding on randomly oriented fractures, leading to a linear increase in deviatoric stress with depth known as Byerlee's Law (Brace and Kohlstedt, 1980; Byerlee, 1978). The shear stress τ to overcome friction is proportional to the stress normal to the plane of fracture:

$$|\tau| = f\sigma_n \tag{D.3}$$

where f is the coefficient of friction, σ_n the effective normal stress is the lithostatic less the fluid pore pressure (usually assumed to be hydrostatic). It gives

$$|\tau| = f(\rho_c - \rho_w)gz \tag{D.4}$$

where ρ_c is the density of rock and ρ_w that of water. Byerlee's experimental data show that:

$$\tau = 0.85\sigma_n \qquad \sigma_n < 200\ MPa \tag{D.5}$$

$$\tau = 50 + 0.6\sigma_n \quad \sigma_n > 200\ MPa \tag{D.6}$$

In horizontal compression, where the maximum principal stress is horizontal σ_h, and the minimum σ_v is vertical, we have:

$$\sigma_h = 5\sigma_v \qquad \sigma_n < 200\ MPa \tag{D.7}$$

$$\sigma_h = 3.1\sigma_v + 175 \qquad \sigma_n > 200\ MPa \tag{D.8}$$

The strength of the crust in the brittle regime is the difference in principal stress components ssnecessary to overcome friction:

$$\sigma = \sigma_h - \sigma_v \tag{D.9}$$

References

Ague, J.J., Eckert, J.O., Chu, X., Baxter, E.F., Chamberlain, C.P., 2012. Discovery of ultrahigh-temperature metamorphism in the Acadian orogen, Connecticut, USA. Geology 41, 271–274.

Andreoli, M.A.G., Hart, R.G., Ashwal, L.D., Coetzee, H., 2006. Correlations between U, Th content and metamorphic grade in the western Namaqualand Belt, South Africa, with implications for radioactive heating of the crust. Journal of Petrology 47, 1095–1118.

Arndt, N.T., Goldstein, S.L., 1989. An open boundary between lower continental crust and mantle: its role in crust formation and crustal recycling. Tectonophysics 161, 201–212.

Artemieva, I., Mooney, W., 2001. Thermal thickness and evolution of Precambrian lithosphere: a global study. Journal of Geophysical Research - Solid Earth 106, 16,387–16,414.

Ashwal, L.D., Morgan, P., Kelley, S.A., Percival, J., 1987. Heat production in an Archean crustal profile and implications for heat flow and mobilization of heat producing elements. Earth and Planetary Science Letters 85, 439–450.

Bassin, C., Laske, G., Masters, G., 2000. The current limits of resolution for surface wave tomography in North America. EOS. Transactions of the American Geophysical Union 81, F897.

Beaumont, C., Jamieson, R.A., Nguyen, M.H., Medvedev, S., 2004. Crustal channel flows: 1. Numerical models with applications to the tectonics of the Himalayan–Tibetan orogen. Journal of Geophysical Research - Solid Earth 109, B06406.
Bedle, H., van der Lee, S., 2009. S velocity variations beneath North America. Journal of Geophysical Research - Solid Earth 114, B07308 Jul.
Birch, F., 1950. Flow of heat from the front range, Colorado. Geological Society of America Bulletin 61, 567–630.
Birch, F., Roy, R.F., Decker, E.R., 1968. Heat flow and thermal history in New England and New York. In: An-Zen, E. (Ed.), Studies of Appalachian Geology. Wiley-Interscience, New York, pp. 437–451.
Bird, P., 1991. Lateral extrusion of lower crust from under high topography in the isostatic limit. Journal of Geophysical Research - Solid Earth 96 (B6), 10275–10286.
Bodorkos, S., Sandiford, M., Minty, B.R., Blewett, R.S., 2004. A high-resolution, calibrated airborne radiometric dataset applied to the estimation of crustal heat production in the Archaean northern Pilbara Craton, Western Australia. Precambrian Research 128 (1), 57–82.
Bott, M., 1989. Plate boundary forces at subduction zones and trench-arc compression. Tectonophysics 170, 1–15.
Boyd, F.R., Gurney, J.J., Richardson, S.H., 1985. Evidence for a 150–200-km thick Archaean lithosphere from diamond inclusion thermobarometry. Nature 315, 387–389.
Brace, W.F., Kohlstedt, D.L., 1980. Limits on lithospheric stress imposed by laboratory experiments. Journal of Geophysical Research 85, 6248–6252.
Brady, R.J., Ducea, M.N., Kidder, S.B., Saleeby, J.B., 2006. The distribution of radiogenic heat production as a function of depth in the Sierra Nevada batholith, California. Lithos 86, 229–244.
Buck, W.R., 1991. Modes of continental lithospheric extension. Journal of Geophysical Research - Solid Earth 96, 20.
Burov, E., Jaupart, C., Mareschal, J.C., 1998. Large-scale crustal heterogeneities and lithospheric strength in cratons. Earth and Planetary Science Letters 164, 205–219.
Byerlee, J.D., 1978. Friction of rocks. Pure and Applied Geophysics 116, 615–626.
Canil, D., 2008. Canada's craton: a bottoms-up view. GSA Today 18 (6), 4.
Carter, N.L., Tsenn, M.C., 1987. Flow properties of continental lithosphere. Tectonophysics 136, 27–63.
Chamberlain, C.P., Sonder, L.J., 1990. Heat-producing elements and the thermal and baric patterns of metamorphic belts. Science 250, 763–769.
Chapman, D., Pollack, H., 1974. 'Cold spot' in West Africa anchoring the African plate. Nature 250, 477–478.
Clark, A., Fitzsimons, C., Healy, D., Harley, S., 2011. How does the continental crust get really hot. Elements 7, 235–240.
Copley, A., Avouac, J.-P., Royer, J.-Y., 2010. India–Asia collision and the Cenozoic slowdown of the Indian plate: implications for the forces driving plate motions. Journal of Geophysical Research - Solid Earth 115 (B3).
Della Vedova, B., Von Herzen, R.P., 1987. Geothermal heat flux at the cost b-2 and b-3 wells, U.S. atlantic continental margin. Tech. Rep. WHOI-87-27, Woods Hole Oceanog. Inst. Tech. Rept.
Duchkov, A.D., 1991. Review of Siberian heat flow data. In: Cermak, V., Rybach, L. (Eds.), Terrestrial Heat Flow and the Lithosphere Structure. Springer-Verlag, Berlin, pp. 426–443.
Durham, W.B., Mirkovich, V.V., Heard, H.C., 1987. Thermal diffusivity of igneous rocks at elevated pressure and temperature. Journal of Geophysical Research - Solid Earth 92, 11615–11634.
Eade, K.E., Fahrig, W.F., 1971. Geochemical Evolutionary Trends of Continental Plates: a Preliminary Study of the Canadian Shield. Geological Survey of Canada Bulletin vol. 179 51 pp.
England, P.C., Thompson, A.B., 1984. Pressure–temperature–time paths of regional metamorphism. I. Heat transfer during the evolution of regions of thickened continental crust. Journal of Petrology 25, 894–928.
Floyd, P.A., Winchester, J.A., Park, R.G., 1989. Geochemistry and tectonic setting of Lewisian clastic metasediments from the early Proterozoic Loch Maree group of Gairloch, NW Scotland. Precambrian Research 45, 203–214.
Foland, K.A., Allen, J.C., 1991. Magma sources for Mesozoic anorogenic granites of the White Mountain magma series, New England USA. Contributions to Mineralogy and Petrology 109, 195–211.
Forsyth, D.W., Uyeda, S., 1975. On the relative importance of the driving forces of plate motions. Geophysical Journal of the Royal Astronomical Society 43, 163–200.
Fountain, D.M., 1986. Is there a relationship between seismic velocity and heat production for crustal rocks? Earth planet. Science Letters 79, 145–150.
Fountain, D.M., Salisbury, M.H., 1981. Exposed cross-sections through the continental crust: implications for crustal structure, petrology, and evolution. Earth and Planetary Science Letters 56, 263–277.
Fountain, D.M., Salisbury, M.H., Furlong, K.P., 1987. Heat production and thermal conductivity of rocks from the Pikwitonei-Sachigo continental cross-section, central Manitoba: implications for the thermal structure of Archean crust. Canadian Journal of Earth Sciences 24, 1583–1594.
Galson, D., 1983. Heat Production in the Ivrea and Strona Ceneri Zones Ph.D. thesis Univ. Cambridge, Cambridge, U.K. 200 pp.
Gaudemer, Y., Tapponnier, P., Jaupart, C., 1988. Thermal control on post-orogenic extension in collision belts. Earth and Planetary Science Letters 89, 48–62.
Grütter, H.S., 2009. Pyroxene xenocryst geotherms: techniques and application. Lithos 112, 1167–1178.
Guillou, L., Mareschal, J.C., Jaupart, C., Gariépy, C., Bienfait, G., Lapointe, R., 1994. Heat flow and gravity structure of the Abitibi belt, Superior Province, Canada. Earth and Planetary Science Letters 122, 447–460.
Hacker, B.R., Mehl, L., Kelemen, P.B., Rioux, M., Behn, M.D., Luffi, P., 2008. Reconstruction of the Talkeetna intraoceanic arc of Alaska through thermobarometry. Journal of Geophysical Research - Solid Earth 113 (B3), B03204.
Hacker, B.R., Kelemen, P.B., Behn, M.D., 2011. Differentiation of the continental crust by relamination. Earth and Planetary Science Letters 307, 501–516.
Hacker, B.R., Kelemen, P.B., Behn, M.D., 2015. Continental lower crust. Annual Review of Earth and Planetary Sciences 43, 6.1–6.39.
Hajnal, Z., Lewry, J., White, D., Ashton, K., Clowes, R., Stauffer, M., Gyorfi, I., Takacs, E., 2005. The Sask Craton and Hearne Province margin: seismic reflection studies in the western Trans-Hudson Orogen. Canadian Journal of Earth Sciences 42, 403–419.
Hasterok, D., Chapman, D.S., 2011. Heat production and geotherms for the continental lithosphere. Earth and Planetary Science Letters 307, 59–70.
Heaman, L.M., Bohm, C.O., Machado, N., Krogh, T.E., Weber, W., Corkery, M.T., 2011. The Pikwitonei granulite domain, Manitoba: a giant Neoarchean high-grade terrane in the northwest Superior Province. Canadian Journal of Earth Sciences 48, 205–245.
Hopper, J.R., Buck, W.R., 1993. The initiation of rifting at constant tectonic force — role of diffusion creep. Journal of Geophysical Research - Solid Earth 98, 16.
Huang, Y., Chubakov, V., Mantovani, F., Rudnick, R.L., McDonough, W.F., 2013. A reference Earth model for the heat-producing elements and associated geoneutrino flux. Geochemistry, Geophysics, Geosystems 14, 2003–2029.
Huerta, A.D., Royden, L.H., Hodges, K.V., 1998. The thermal structure of collisional orogens as a response to accretion, erosion, and radiogenic heating. Journal of Geophysical Research - Solid Earth 103, 15.
Hyndman, R.D., 2010. The consequences of Canadian Cordillera thermal regime in recent tectonics and elevation: a review. Canadian Journal of Earth Sciences 47, 621–632.
Jagoutz, O.E., 2010. Construction of the granitoid crust of an island arc. Part II: a quantitative petrogenetic model. Contributions to Mineralogy and Petrology 160, 359–381 Sep.
Jagoutz, O.E., Schmidt, M., 2012. The formation and bulk composition of modern juvenile continental crust: the Kohistan arc. Chemical Geology 298-299, 79–96.
Jaupart, C., 1983. Horizontal heat transfer due to radioactivity contrasts: causes and consequences of the linear heat flow-heat production relationship. Geophysical Journal of the Royal Astronomical Society 75, 411–435.
Jaupart, C., Mareschal, J.C., 1999. The thermal structure and thickness of continental roots. Lithos 48, 93–114.
Jaupart, C., Mareschal, J.C., 2011. Heat Generation and Transport in the Earth. Cambridge University Press, Cambridge (U.K.).
Jaupart, C., Mareschal, J.C., 2014. In: Rudnick, R.L. (Ed.), Constraints on Crustal Heat Production from Heat Flow Data, 2nd edition Treatise on Geochemistry, The Crust vol. 4. Elsevier, New York, pp. 53–73.
Jaupart, C., Mareschal, J.C., 2015a. Heat flow and thermal structure of the lithosphere. In: Watts, A.B. (Ed.), Treatise on Geophysics, 2nd edition The Lithosphere vol. 6. Elsevier, pp. 217–253.
Jaupart, C., Mareschal, J.-C., 2015b. Post-orogenic thermal evolution of newborn Archean continents. Earth and Planetary Science Letters 432, 36–45 Dec.
Jaupart, C., Mann, J.R., Simmons, G., 1982. A detailed study of the distribution of heat flow and radioactivity in New Hampshire (U.S.A.). Earth and Planetary Science Letters 59, 267–287.
Jaupart, C., Mareschal, J.C., Guillou-Frottier, L., Davaille, A., 1998. Heat flow and thickness of the lithosphere in the Canadian Shield. Journal of Geophysical Research - Solid Earth 103, 15269–15286.
Jaupart, C., Mareschal, J.-C., Bouquerel, H., Phaneuf, C., 2014. The building and stabilization of an Archean Craton in the Superior Province, Canada, from a heat flow perspective. Journal of Geophysical Research - Solid Earth 119, 9130–9155.
Jaupart, C., Labrosse, S., Lucazeau, F., Mareschal, J.C., 2015. Temperatures, heat and energy in the mantle of the earth. In: Bercovici, D. (Ed.), Treatise on Geophysics. The Mantle vol. 7. Elsevier, New York, pp. 223–270.
Jeffreys, H., 1936. On the radioactivities of rocks. Beitrage zur Geophysik 47, 149–170.
Joeleht, T.H., Kukkonen, I.T., 1998. Thermal properties of granulite facies rocks in the Precambrian basement of Finland and Estonia. Tectonophysics 291, 195–203.
Johnson, T., White, R., 2011. Phase equilibrium constraints on conditions of granulite facies metamorphism at Scourie, NW Scotland. Journal of the Geological Society of London 168, 147–158.
Jones, M.Q.W., 1987. Heat flow and heat production in the Namaqua mobile belt, South Africa. Journal of Geophysical Research - Solid Earth 92, 6273–6289.
Jones, M.Q.W., 1992. Heat flow anomaly in Lesotho: implications for the southern boundary of the Kaapvaal craton. Geophysical Research Letters 19, 2031–2034.
Jull, M., Kelemen, P.B., 2001. On the conditions for lower crustal convective instability. Journal of Geophysical Research - Solid Earth 106, 6423–6446.
Kelemen, P., Hanghoj, K., Greene, A., 2014. One view of the geochemistry of subduction-related magmatic arcs, with an emphasis on primitive andesite and lower crust. In: Rudnick, R.L. (Ed.), The Crust, 2nd edition Treatise on Geochemistry vol. 4. Elsevier-Permagon, Oxford, pp. 749–805.
Kinnaird, T., Prave, A.R., Kirkland, C., Horstwood, M., Parrish, R., Batchelor, R., 2007. The late Mesoproterozoic–early Neoproterozoic tectonostratigraphic evolution of NW Scotland: the Torridonian revisited. Journal of the Geological Society of London 164, 541–551.
Kramers, J., Kreissig, K., Jones, M., 2001. Crustal heat production and style of metamorphism: a comparison between two high-grade provinces in the Limpopo Belt, South Africa. Precambrian Research 112, 149–163.
Krogh, T.E., 1993. High precision U–Pb ages for granulite metamorphism and deformation in the Archean Kapuskasing structural zone, Ontario: implications for structure and development of the lower crust. Earth and Planetary Science Letters 119, 1–18.
Kukkonen, I.T., 1989. Terrestrial heat flow and radiogenic heat production in Finland, the central Baltic Shield. Tectonophysics 164, 219–230.
Kukkonen, I.T., Jõeleht, A., 1996. Geothermal modelling of the lithosphere in the central Baltic Shield and its southern slope. Tectonophysics 255, 25–45.
Kukkonen, I.T., Peltonen, P., 1999. Xenolith-controlled geotherm for the central Fennoscandian shield: implications for lithosphere–asthenosphere relations. Tectonophysics 304, 301–315.

Kukkonen, I., Peltoniemi, S., 1998. Relationships between thermal and other petrophysical properties of rocks in Finland. Physics of the Earth and Planetary Interiors 23, 341–349.
Kukkonen, I.T., Golovanova, Y.V., Druzhinin, V.S., Kosarev, A.M., Schapov, V.A., 1997. Low geothermal heat flow of the Urals fold belt: implication of low heat production, fluid circulation or paleoclimate. Tectonophysics 276, 63–85.
Kumar, P.S., Reddy, G.K., 2004. Radioelements and heat production of an exposed Archaean crustal cross-section, Dharwar craton, south India. Earth and Planetary Science Letters 224, 309–324.
Kumar, P.S., Menon, R., Reddy, G.K., 2007. The role of radiogenic heat production in the thermal evolution of a Proterozoic granulite-facies orogenic belt: Eastern Ghats, Indian shield. Earth and Planetary Science Letters 254, 39–54.
Kumar, P.S., Menon, R., Reddy, G.K., 2009. Heat production heterogeneity of the Indian crust beneath the Himalaya: Insights from the northern Indian shield. Earth and Planetary Science Letters 283, 190–196.
Kutas, R.I., 1977. Investigation of heat flow in the territory of the Ukraine. Tectonophysics 41, 139–145.
Lambert, I.B., Heier, K.S., 1967. The vertical distribution of uranium, thorium, and potassium in the continental crust. Geochimica et Cosmochimica Acta 31, 377–390.
Landstrom, O., Larson, S.A., Lind, G., Malmqvist, D., 1980. Geothermal investigations in the Bohus granite area in southwestern Sweden. Tectonophysics 64, 131–162.
Laske, G., Masters, G., Ma, Z., Pasyanos, M., 2013. Update on Crust1.0 — a 1-degree Global Model of Earth's Crust. Geophysical Research Abstracts vol. 15. EGU.
Lee, C.-T.A., Morton, D., Kistler, R.W., Baird, A.K., 2007. Petrology and tectonics of phanerozoic continent formation: from island arcs to accretion and continental arc magmatism. Earth and Planetary Science Letters 263, 370–387.
Lévy, F., Jaupart, C., 2011. Temperature and rheological properties of the mantle beneath the North American craton from an analysis of heat flux and seismic data. Journal of Geophysical Research - Solid Earth 116 (B15), 1408.
Lévy, F., Jaupart, C., Mareschal, J., Bienfait, G., Limare, A., 2010. Low heat flux and large variations of lithospheric thickness in the Canadian Shield. Journal of Geophysical Research - Solid Earth 115, 6404.
Lewis, T.J., Hyndman, R.D., Fluck, P., 2003. Heat flow, heat generation and crustal temperatures in the northern Canadian Cordillera: thermal control on tectonics. Journal of Geophysical Research - Solid Earth 108, 2316.
Lyons, J.B., 1964. Distribution of thorium, uranium in three early Paleozoic plutonic suites of New Hamphsire. Tech. Rep. 1144-F, U.S. Geological Survey Bulletin.
Mareschal, J.C., Jaupart, C., 2006. Archean thermal regime and stabilization of the cratons. In: Benn, K., Condie, K., Mareschal, J.C. (Eds.), Archean Geodynamic Processes. AGU, Washington (DC), pp. 61–73.
Mareschal, J.C., Jaupart, C., 2004. Variations of surface heat flow and lithospheric thermal structure beneath the North American craton. Earth and Planetary Science Letters 223, 65–77.
Mareschal, J.-C., Jaupart, C., 2013. Radiogenic heat production, thermal regime and evolution of continental crust. Tectonophysics 609, 524–534.
Mareschal, J.C., Jaupart, C., Gariépy, C., Cheng, L.Z., Guillou-Frottier, L., Bienfait, G., Lapointe, R., 2000a. Heat flow and deep thermal structure near the southeastern edge of the Canadian Shield. Canadian Journal of Earth Sciences 37, 399–414.
Mareschal, J.C., Poirier, A., Rolandone, F., Bienfait, G., Gariépy, C., Lapointe, R., Jaupart, C., 2000b. Low mantle heat flow at the edge of the North American Continent, Voisey Bay, Labrador. Geophysical Research Letters 27, 823–826.
McKenzie, D., 1977. The initiation of trenches: a finite amplitude instability. In: Talwani, M., Pitman, W. (Eds.), Island Arcs, Deep Sea Trenches and Back-Arc Basins. Vol. 1 of Maurice Ewing Series. American Geophysical Union, Washington, DC, pp. 57–61.
McKenzie, D., Priestley, K., 2016. Speculations on the formation of cratons and cratonic basins. Earth and Planetary Science Letters 435, 94–104.
McKenzie, D., Nimmo, F., Jackson, J.A., Gans, P., Miller, E., 2000. Characteristics and consequences of flow in the lower crust. Journal of Geophysical Research 105 (B5), 11–029.
McLaren, S., Sandiford, M., Hand, M., Neumann, N., Wyborn, L., Bastrakova, I., 2003. The hot southern continent: heat flow and heat production in Australian Proterozoic terranes. In: Hillis, R.R., Müller, R.D. (Eds.), Evolution and Dynamics of the Australian Plate. Geological society of Australia Special Publications, Ch. 12 vol. 22, pp. 151–161.
McLaren, S., Sandiford, M., Powell, R., Neumann, N., Woodhead, J., 2006. Palaeozoic intraplate crustal anatexis in the Mount Painter Province, South Australia: timing, thermal budgets and the role of crustal heat production. Journal of Petrology 47 (12), 2281–2302.
Meldrum, A., Abdel-Rahman, A.F.M., Martin, R., Wodicka, N., 1997. The nature, age and petrogenesis of the Cartier Batholith, northern flank of the Sudbury Structure, Ontario, Canada. Precambrian Research 82, 165–285.
Merriman, J.D., Li, A.G.W., Hofmeister, A.M., Nabelek, P.I., Benn, K., 2013. Thermal transport properties of major Archean rock types to high temperature and implications for cratonic geotherms. Precambrian Research 233, 358–372.
Mezger, K., Bohlen, S., Hanson, G.N., 1990. Metamorphic history of the Archean Pikwitonei granulite domain and the cross Lake subprovince, Superior Province, Manitoba, Canada. Journal of Petrology 32, 483–517.
Miao, S.Q., Li, H.P., Chen, G., 2014. Temperature dependence of thermal diffusivity, specific heat capacity and thermal conductivity for several types of rocks. Journal of Thermal Analysis and Calorimetry 115, 1057–1063.
Michaut, C., Jaupart, C., 2007. Secular cooling and thermal structure of continental lithosphere. Earth and Planetary Science Letters 257, 83–96.
Michaut, C., Jaupart, C., Bell, D.R., 2007. Transient geotherms in Archean continental lithosphere: new constraints on thickness and heat production of the subcontinental lithospheric mantle. Journal of Geophysical Research - Solid Earth 112, 4408.
Michaut, C., Jaupart, C., Mareschal, J.C., 2009. Thermal evolution of cratonic roots. Lithos 109, 47–60.
Mooney, W.D., Laske, G., Guy Masters, T., 1998. Crust 5.1: a global crustal model at 5° × 5°. Journal of Geophysical Research - Solid Earth 103, 727–748.
Morgan, P., 1985. Crustal radiogenic heat production and the selective survival of ancient continental crust. Journal of Geophysical Research - Solid Earth 90, C561–C570.
Musacchio, G., White, D.J., Asudeh, I., Thomson, C.J., 2004. Lithospheric structure and composition of the Archean western Superior Province from seismic refraction/wide-angle reflection and gravity modeling. Journal of Geophysical Research - Solid Earth 109 (B18), 3304.
Neumann, N., Sandiford, M., Foden, J., 2000. Regional geochemistry and continental heat flow: implications for the origin of the South Australian heat flow anomaly. Earth and Planetary Science Letters 183, 107–120.
Nicolaysen, L.O., Hart, R.J., Gale, N.H., 1981. The Vredefort radioelement profile extended to supracrustal strata at Carletonville, with implications for continental heat flow. Journal of Geophysical Research - Solid Earth 86, 10653–10662.
Nielsen, S.B., 1987. Steady state heat flow in a random medium and the linear heat flow–heat production relationship. Geophysical Research Letters 14, 318–322.
Nyblade, A.A., Pollack, H.N., 1993. A global analysis of heat flow from Precambrian terrains — implications for the thermal structure of Archean and Proterozoic lithosphere. Journal of Geophysical Research - Solid Earth 98, 12207–12218.
Park, R.G., Tarney, J., Connelly, J.N., 2001. The Loch Maree Group: palaeoproterozoic subduction accretion complex in the Lewisian of NW Scotland. Precambrian Research 105, 205–226.
Parsons, B., Richter, F.M., 1980. A relation between the driving force and geoid anomaly associated with mid-ocean ridges. Earth and Planetary Science Letters 51, 445–450.
Percival, J.A., West, G.F., 1994. The Kapuskasing uplift: a geological and geophysical synthesis. Canadian Journal of Earth Sciences 31, 1256–1286.
Perry, H.K.C., Eaton, D.W.S., Forte, A.M., 2002. A revised crustal model for Canada based on Lithoprobe results. Geophysical Journal International 150, 285–294.
Perry, H.K.C., Jaupart, C., Mareschal, J.C., Bienfait, G., 2006a. Crustal heat production in the Superior Province, Canadian Shield, and in North America inferred from heat flow data. Journal of Geophysical Research - Solid Earth 111, B04401.
Perry, H.K.C., Jaupart, C., Mareschal, J.-C., Shapiro, N.M., 2006b. Upper mantle velocity-temperature conversion and composition determined from seismic refraction and heat flow. Journal of Geophysical Research - Solid Earth 111, B07301.
Perry, H., Rosieanu, C., Mareschal, J.C., Jaupart, C., 2010. Thermal regime of the lithosphere in Canada. Canadian Journal of Earth Sciences 47, 389–408.
Phaneuf, C., Mareschal, J., 2014. Estimating concentrations of heat producing elements in the crust near the Sudbury Neutrino Observatory, Ontario, Canada. Tectonophysics 622, 135–144.
Pinet, C., Jaupart, C., 1987. The vertical distribution of radiogenic heat production in the Precambrian crust of Norway and Sweden: geothermal implications. Geophysical Research Letters 14, 260–263.
Pinet, C., Jaupart, C., Mareschal, J.-C., Gariepy, C., Bienfait, G., Lapointe, R., 1991. Heat flow and structure of the lithosphere in the eastern Canadian shield. Journal of Geophysical Research - Solid Earth 96, 19941–19963.
Pollack, H.N., Chapman, D.S., 1977. On the regional variation of heat flow, geotherms and thickness of the lithosphere. Tectonophysics 38, 279–296.
Pysklywec, R.N., Beaumont, C., 2004. Intraplate tectonics: feedback between radioactive thermal weakening and crustal deformation driven by mantle lithosphere instabilities. Earth and Planetary Science Letters 221, 275–292.
Ranalli, G., 1995. Rheology of the Earth. 2nd edition. Chapman Hall, London.
Rey, P.F., Coltice, N., 2008. Neoarchean lithospheric strengthening and the coupling of Earth's geochemical reservoirs. Geology 36, 635–638.
Rogers, J.J.W., Adams, J.A.S., Gatlin, B., 1965. Distribution of thorium, uranium and potassium in three cores from the Conway granite, New Hampshire. AJS 263, 817–822.
Rolandone, F., Jaupart, C., Mareschal, J.C., Gariépy, C., Bienfait, G., Carbonne, C., Lapointe, R., 2002. Surface heat flow, crustal temperatures and mantle heat flow in the Proterozoic Trans-Hudson Orogen, Canadian Shield. Journal of Geophysical Research - Solid Earth 107, 2314.
Rollinson, H., 2012. Geochemical constraints on the composition of Archean lower continental crust: partial melting in the Lewisian granulites. Earth and Planetary Science Letters 351-352, 1–12.
Roy, S., Rao, R.U.M., 2000. Heat flow in the Indian shield. Journal of Geophysical Research - Solid Earth 105, 25587–25604.
Roy, S., Rao, R.U.M., 2003. Towards a crustal thermal model for the Archean Dharwar craton, southern India. Physics and Chemistry of the Earth 28, 361–373.
Roy, R.F., Blackwell, D.D., Birch, F., 1968. Heat generation of plutonic rocks and continental heat flow provinces. Earth and Planetary Science Letters 5, 1–12.
Rudnick, R.L., Fountain, D.M., 1995. Nature and composition of the continental crust: a lower crustal perspective. Reviews of Geophysics 33, 267–309.
Rudnick, R.L., Gao, S., 2014. In: Rudnick, R.L. (Ed.), Composition of the Continental Crust, 2nd edition. Treatise on Geochemistry vol. 4, pp. 1–51.
Rudnick, R.L., Nyblade, A.A., 1999. The thickness of Archean lithosphere: constraints from xenolith thermobarometry and surface heat low. In: Fei, Y., Bertka, C.M., Mysen, B.O. (Eds.), Mantle Petrology; Field Observations and High Pressure Experimentation: a Tribute to Francis R. (Joe) Boyd. Geochemical Society, Kansas-City (MO), pp. 3–11.
Rudnick, R., Taylor, S., 1987. The composition and petrogenesis of the lower crust: a xenolith study. Journal of Geophysical Research - Solid Earth 92 (B13), 13981–14005.
Russell, J.K., Dipple, G.M., Kopylova, M.G., 2001. Heat production and heat flow in the mantle lithosphere, Slave craton, Canada. Physics of the Earth and Planetary Interiors 123, 27–44.
Saltus, R.W., Lachenbruch, A.H., 1991. Thermal evolution of the sierra Nevada: tectonic implications of new heat flow data. Tectonics 10, 325–344.
Sand, K.K., Waight, T.E., Pearson, D.G., Nielsen, T.F., Makovicky, E., Hutchison, M.T., 2009. The lithospheric mantle below southern West Greenland: a geothermobarometric approach to diamond potential and mantle stratigraphy. Lithos 112, 1155–1166.

Sandiford, M., Hand, M., 1998. Controls on the locus of intraplate deformation in central Australia. Earth and Planetary Science Letters 162, 97–110.
Sandiford, M., McLaren, S., 2002. Tectonic feedback and the ordering of heat producing elements within the continental lithosphere. Earth and Planetary Science Letters 204, 133–150.
Sandiford, M., McLaren, S., Neuman, N., 2002. Long term thermal consequences of the redistribution of heat producing elements associated with large-scale granitic complexes. Journal of Metamorphic Geology 20, 87–98.
Sawka, W.N., Chappell, B.W., 1988. Fractionation of uranium, thorium and trace elements in a vertically zoned granidiorite: implications for heat production distributions in the Sierra Nevada batholith, California, U.S.A. Geochimica et Cosmochimica Acta 52, 1131–1143.
Slagstad, T., 2008. Radiogenic heat production of Archean to Permian geological provinces in Norway. Norwegian Journal of Geology 88, 149–166.
Slagstad, T., Balling, N., Elvebakk, H., Midttømme, K., Olesen, O., Olsen, L., Pascal, C., 2009. Heat-flow measurements in Late Palaeoproterozoic to Permian geological provinces in south and central Norway and a new heat-flow map of Fennoscandia and the Norwegian-Greenland Sea. Tectonophysics 473, 341–361.
Tammemagi, S.R., Smith, N., 1975. A radiogeologic study of the granites of SW England. Journal of the Geological Society of London 131, 415–427.
Taylor, S.R., 1977. The origin and growth of continents. Tectonophysics 4, 17–34.
Taylor, S.R., McLennan, S.M., 1995. The Continental Crust: its Composition and Evolution. Blackwell.
Thompson, P.H., Judge, A.S., Lewis, T.J., 1995. Thermal parameters in rock units of the Winter Lake-Lac de Gras area, central Slave Province, Northwest Territories—implications for diamond genesis. Current Research 1995-E, 125–135.
Tommasi, A., Vauchez, A., 2001. Continental rifting parallel to ancient collisional belts: an effect of the mechanical anisotropy of the lithospheric mantle. Earth and Planetary Science Letters 185 (1), 199–210.
Vasseur, G., Singh, R.N., 1986. Effects of random horizontal variations in radiogenic heat source distribution on its relationship with heat flow. Journal of Geophysical Research - Solid Earth 91, 10397–10404.
Vauchez, A., Tommasi, A., Barruol, G., 1998. Rheological heterogeneity, mechanical anisotropy and deformation of the continental lithosphere. Tectonophysics 296 (1), 61–86.
Webb, P.C., Lee, M.K., Brown, G.C., 1987. Heat flow–heat production relationships in the UK and the vertical distribution of heat production in granite batholiths. Geophysical Research Letters 14, 279–282.
Yang, X., Li, Z., Wang, H., Chen, H., Li, Y., Xiao, W., 2015. Petrology and geochemistry of ultrahigh-temperature granulites from the South Altay origenic belt, northwestern China: implications for metamorphic evolution and protolith composition. Island Arc 24, 169–187.
Young, G.M., 1999. Some aspects of the geochemistry, provenance and paleoclimatology of the Torridonian of NW Scotland. Journal of the Geological Society of London 156, 1097–1111.